

AD-A034 938

AIR FORCE INST OF TECH WRIGHT-PATTERSON AFB OHIO SCH--ETC F/G 20/11
COMPARING TRIGONOMETRIC AND CONVENTIONAL FINITE DIFFERENCE APPR--ETC(U)
DEC 76 W H DESCHLER

UNCLASSIFIED

GAE/MC/76D-3

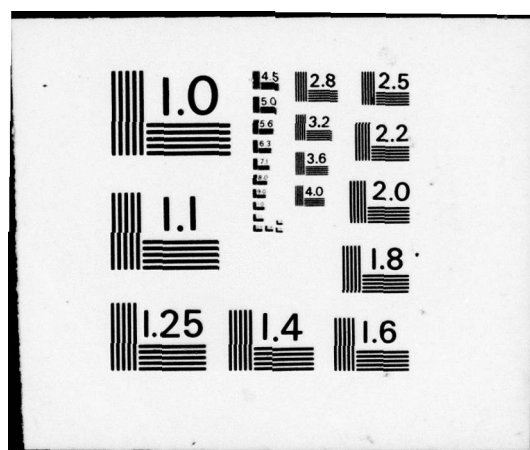
NL

1 OF 1
ADA034938

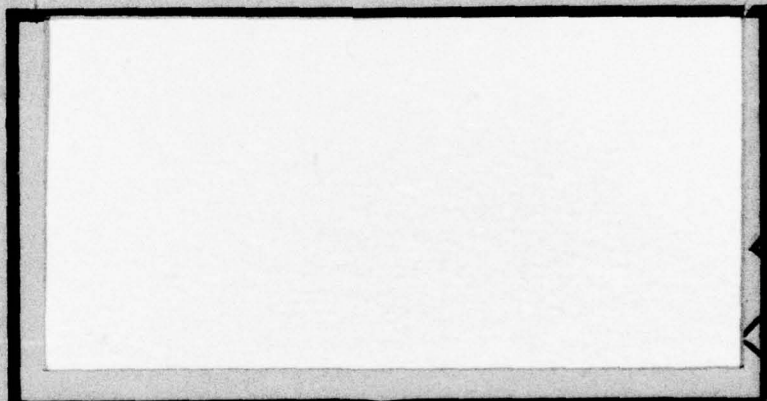


END

DATE
FILMED
3 - 77



ADA 034938



UNITED STATES AIR FORCE
AIR UNIVERSITY
AIR FORCE INSTITUTE OF TECHNOLOGY
Wright-Patterson Air Force Base, Ohio

DISTRIBUTION STATEMENT A
Approved for public release
Distribution Unlimited

GAE/MC/76D-3



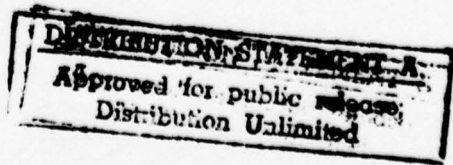
COMPARING TRIGONOMETRIC AND CONVENTIONAL
FINITE DIFFERENCE APPROXIMATIONS FOR
PLATE BUCKLING

THESIS

GAE/MC/76D-3

William H. Deschler
Captain USAF

ACCESSION NO.	
RTS	<input checked="" type="checkbox"/> White Section
DRC	<input type="checkbox"/> Bell Section
UNCLASSIFIED	
JUSTIFICATION	
BY	
DISTRIBUTION/AVAILABILITY CODES	
Ref.	AVAIL. AND/OR SPECIAL
A	



(14)

GAE/MC/76D-3

(6)

COMPARING TRIGONOMETRIC AND CONVENTIONAL
FINITE DIFFERENCE APPROXIMATIONS FOR
PLATE BUCKLING

(9)

Master's
THESIS

Presented to the Faculty of the School of Engineering
of the Air Force Institute of Technology
Air University
in Partial Fulfillment of the
Requirements for the Degree of
Master of Science

(10)

William H. Deschler

Captain

USAF

Graduate Aeronautical Engineering

(11)

Dec 1976

(12) 7-P.

Approved for public release, distribution unlimited.

012225

YB

Preface

This thesis is the result of my efforts to compare buckling coefficients determined by trigonometric and conventional finite difference methods incorporating both "virtual work and equilibrium equations. It is hoped that the results of this study will aid the engineering community in deciding the value of trigonometric finite difference approximations.

I am especially indebted to Dr. Anthony Palazotto for suggesting this topic. This very knowledgeable man made himself available at all hours and shared a delightful sense of humor with me that made the learning effort an enjoyable experience.

I want to thank my beautiful wife, Georgia, and lovely girls, Gigi and Angie for their love, patience, and encouragement throughout this educational endeavor.

A special thanks to Jerry Bennington, Jr. for allowing me to use his tape recorder to preserve many of the valuable ideas discussed with Dr. Palazotto.

William H. Deschler

Contents

Preface	ii
List of Figures	iv
Symbols	vi
Abstract	viii
I. Introduction	1
Background	1
Purpose	3
General Procedure	3
II. Theory	5
Assumptions	5
Governing Equations	5
III. Numerical Technique	8
Basic Approach	8
Half-Station versus Full-Station	9
Trigonometric versus Polynomial	12
Mesh Arrangement in the Virtual Work Equation	16
Finite Difference Approximation of the Equilibrium Equation	23
IV. Numerical Results	25
Introduction	25
Various Aspect Ratios - Simple Support	26
Various Aspect Ratios - Clamped	26
Degrees of Freedom versus Error - Simple Support	27
Degrees of Freedom versus Error - Clamped	30
V. Conclusions	46
Bibliography	48
Appendix A: Development of Virtual Work Equation . .	51
Appendix B: Factoring Techniques	55
Vita	59

List of Figures

Figure	Page
2.1 Forces and Moments Acting on Differential Element $dx dy$	7
3.1 Finite Difference Grid	10
3.2 Half-station Finite Difference Grid	10
3.3 Function $g(x)$ and a parabola P	13
3.4 Grid Arrangement	19
3.5 Half-station Differences of $w_{,y}$ and $\delta w_{,x}$	20
3.6 The Position of a Reference Point to Evaluate a Mixed Derivative	21
3.7 Computational Model	24
4.a Long Plate Theory	28
4.b $\lambda_x/A = 1$	28
4.c A Lambda Value Displacement Function	30
4.d Long Plate Theory Displacement Function	30
4.e Assumption Versus Actual Wavelength in a Clamped Plate	31
4.1 Finite Difference Approximations	34
4.2 Finite Difference Approximations	35
4.3 Simple Supported Plate $A/B = 0.5$	36
4.4 Simple Supported Plate $A/B = 1.0$	37
4.5 Simple Supported Plate $A/B = 2.0$	38
4.6 Simple Supported Plate $A/B = 3.0$	39
4.7 Simple Supported Plate $A/B = 5.0$	40
4.8 Clamped Plate $A/B = 0.5$	41
4.9 Clamped Plate $A/B = 1.0$	42
4.10 Clamped Plate $A/B = 2.0$	43

4.11	Clamped Plate A/B = 3.0	44
4.12	Clamped Plate A/B = 5.0	45

Symbols

- A dimension of a plate parallel to x-direction
- A_{ij} curvature terms defined in Equation (3-54)
- B dimension of a plate parallel to y-direction
- C_{ij} plate stiffness terms defined by Equation (3-53)
- D isotropic plate flexural stiffness
- $D_{11}, D_{12}, D_{22}, D_{66}$ orthotropic plate flexural stiffness
- e_x, e_y, e_{xy} strains
- g represents a function
- g' represents the first derivative of function g
- h mesh size
- h_x mesh size, x-direction
- h_y mesh size, y-direction
- \hat{h}_x, \hat{h}_y trigonometric finite difference terms defined by Equation (3-29)
- i, j indices attached to a variable (may refer to a variable being evaluated at either full- or half-stations, depending on variable) (Fig 4.3)
- I_1, I_3 row designation of boundaries ① and ③ Fig 3.4
- J_2, J_4 column designation of boundaries ② and ④ Fig 3.4
- M, N total number of rows and columns of finite difference stations
- M_x, M_y, M_{xy} bending moments in plate Fig 2.1
- N_x in-plane load Fig 2.1
- P polynomial equation
- Q shear Fig 2.1
- t thickness of plate
- U strain energy

u, v, w displacements in x -, y -, z -directions, respectively

V total potential energy

w_x first partial of w with respect to x

w_{xx} second partial of w with respect to x

x, y plate coordinates Fig 3.4

β ratio of plate width to buckle length for an infinitely long plate

δU internal virtual work

δV virtual work

λ_x, λ_y trigonometric parameters defined through Equation (3-29)

ν Poisson's ratio

$\xi_x \xi_y \eta_x \eta_y$ functions defined by Equations (3-41) - (3-44)

Abstract

Finite difference methods for plate buckling were investigated for various two-dimensional plates. The plates were clamped and simply supported. The rate of convergence to buckling coefficients, considering virtual work and equilibrium, have been compared. A trigonometric function (based on long plate theory) was incorporated into the finite difference approximations of the virtual work expression. Additional trigonometric parameters were also considered in the virtual work equation. Little difference in accuracy was found between results obtained from conventional (polynomial) virtual work versus the equilibrium approach. Noticeable improvement is obtained by using a trigonometric function (long plate assumption) in the virtual work expression. If one varies the trigonometric function (not based on long plate theory), a band of results is created from use of the virtual work equation. Inaccuracies occurred at low degrees of freedom, for clamped plates at all length to width ratios, due to insufficient representation of the boundaries. Two dominant reasons for poor boundary representation seem to be, large mesh size at low degrees of freedom (mesh sizes were held constant) and the trigonometric function (polynomial for conventional finite difference) failing to satisfy the kinematic boundary conditions.

COMPARING TRIGONOMETRIC AND CONVENTIONAL
FINITE DIFFERENCE APPROXIMATIONS FOR
PLATE BUCKLING

I. Introduction

Background

The plate is one of the most effective aerospace structural elements. Many plate characteristics are associated with thinness, thus thinness becomes an important criteria for optimizing the weight considerations of the overall structure. The concern for optimization involves stress calculations which consider equilibrium. Such calculations are not in themselves the end results, for an analyst must go one step further and determine the buckling parameters of the plate structure. This thesis deals with a numerical approach to plate buckling using a recently developed finite difference technique [1].

The theoretical buckling stress of a flat plate is the stress at which an exchange of stable equilibrium occurs between the straight and slightly bent form of the plate. It marks the region where continued load application accelerates the growth of deflections perpendicular to the plane of the plate. The importance of this stability condition lies in the fact that buckling initiates the processes leading to plate failure [2]. Because of the necessity to

incorporate difficult boundary conditions [3], very few plate buckling problems of a practical engineering nature have been solved by the so-called classical techniques (series solution). Apparently the earliest solution to a flat plate stability problem was presented by Bryan [4] in 1891 [5]. Since then, many additional solution techniques have been developed including Navier Solutions [6], use of Fourier Series in the energy equation [7], Galerkins Method, and other approaches [8-14]. All are used to derive approximate answers, but they are lengthy and tedious techniques. The advent of the high-speed computer and subsequent rapid development of numerical methods has allowed the engineer the opportunity to address more precise conceptual representations of actual physical structures.

The succeeding sections of this thesis are directed towards the development of numerical approaches to buckling using a CDC6600 computer. The most efficient numerical technique, referred to as rapid convergence, is defined herein as that technique which provided useful answers incorporating the fewest degrees of freedom. Rapid convergence is a definite concern for buckling considerations.

The evaluation of the convergence rate developed from finite difference approximations in which the buckling mode shape characteristics are incorporated into analogous grid spacing is of prime interest. These characteristics were presented by M. Stein and J. Housner in 1975 [1] when they introduced a trigonometric finite difference procedure. A

comparison between the new trigonometric technique and the finite difference approximation using the common equilibrium equation is presented in this thesis.

Purpose

The purpose of this thesis is to compare buckling coefficients determined by trigonometric and conventional finite difference methods for two-dimensional plates, incorporating both virtual work and equilibrium equations. The development of rapid convergence is of primary interest.

General Procedure

In the approach followed, the virtual work equation was evaluated using finite difference approximations of partial derivatives. This required the separation of a plate's domain into given sets of nodes which were then used in determining each partial derivative expression. Results were then placed into the virtual work equation. Integration was performed leading to the solution of a set of algebraic expressions. Simple support and clamped boundary conditions were investigated. Each plate's aspect ratio (length/width=A/B) was varied from 0.5 to 5. Previous work [1] presented the results for trigonometric finite difference considering square plates and very long plates ($A/B=5$). This thesis considered the borderline between plate and slab theory by investigating aspect ratios of 2 and 3. Solutions for both trigonometric and conventional finite difference approximations of the virtual

work equation have been obtained and compared to the conventional finite difference approximations of the equilibrium equation.

II. Theory

Assumptions

The buckling analysis of rectangular plates has been carried out with the following assumptions.

1. Linear Theory of Elasticity [6,15,16]
 - a) Plane sections remain plane.
 - b) All displacements are related to the middle surface.
 - c) The plate is perfectly flat prior to buckling.
2. Isotropic material
3. Homogeneous material
4. In-plane load $N_x = \text{constant}$ and $N_{xy} = N_y = 0$
5. The nonlinear strain-displacement relationships used to obtain the virtual work equation are

$$\begin{aligned} e_x &= u_{,x} + \frac{1}{2}(w_{,x})^2 \\ e_y &= v_{,y} + \frac{1}{2}(w_{,y})^2 \\ e_{xy} &= u_{,y} + v_{,x} + w_{,x}w_{,y} \end{aligned} \tag{2-1}$$

where e_x , e_y , and e_{xy} are the strains and u , v , and w are the displacements in the x -, y -, and z - directions, respectively [15]. The virtual work equation is developed in Appendix A.

6. Thickness of plate is constant and the plate is thin.

Governing Equations

Equilibrium Differential Equation. The general form

of the differential equation describing the slightly bent equilibrium configuration of an initially flat plate was derived by Stowell [17] and reduced to equation (2-2) for the elastic case in reference [2].

$$\nabla^4 w = -\frac{t}{D}(\sigma_{xw,xx} + 2\sigma_{xyw,xy} + \sigma_{yw,yy}) \quad (2-2)$$

$$-t\sigma_x = N_x \quad t\sigma_{xy} = N_{xy} = 0 \quad t\sigma_y = N_y = 0 \quad (2-3)$$

The force N_x in the plane of the plate is assumed constant (assumption No. 4) and is thus not dependent on the deflection nor is it a function of displacement. This makes equation (2-2) linear. Hence it becomes

$$D\nabla^4 w = N_{xw,xx} \quad (2-4)$$

where D is the flexural rigidity. Equation (2-5) defines D for an isotropic homogeneous material.

$$D = Et^3/12(1-\nu^2) \quad (2-5)$$

Virtual Work Equation. The virtual work of the plate during buckling may be expressed as

$$\delta U = \delta V \quad (2-6)$$

where

$$\delta U = \int_0^b \int_0^a (M_{xw,xx} \delta w + M_{yw,yy} \delta w + 2M_{xyw,xy} \delta w) dx dy \quad (2-7)$$

$$\delta V = \int_0^a \int_0^b (N_{xw,x} \delta w) dy dx \quad (2-8)$$

The sign conventions of the bending moments are given in figure 2-1. Equation (2-6) is developed in Appendix A.

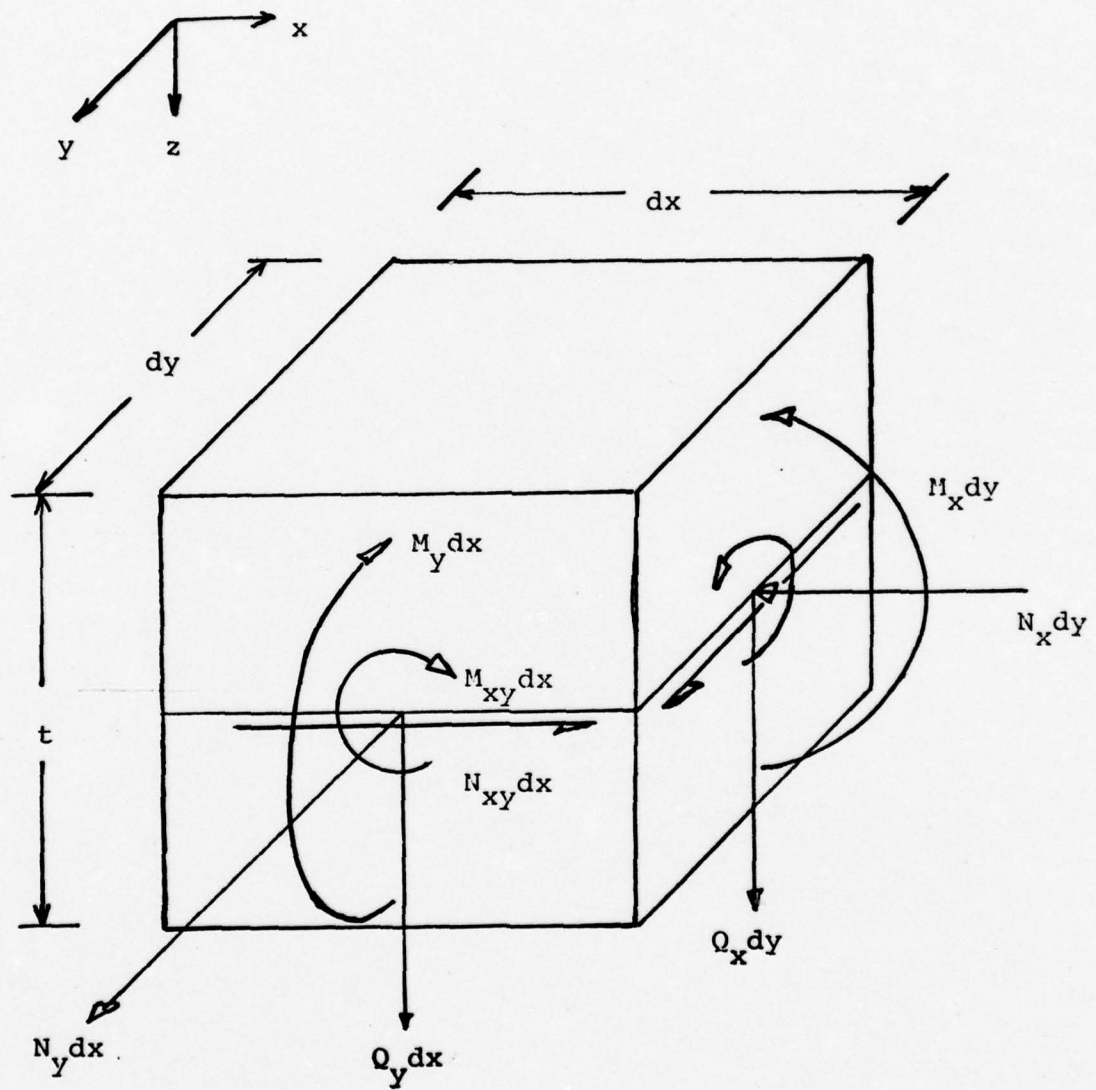


Fig 2.1 Forces and Moments Acting on Differential Element $dx dy$.

III. Numerical Techniques

In the nineteenth century, Boole and others formalized the finite difference method for solving differential equations [5], thus providing the means to reduce the continuum to a system with finite degrees of freedom. Mario G. Salvadori in 1949 [18] presented a comprehensive paper concerning the difference method and applicable extrapolation procedures. Presently, many excellent texts [19-25] may be found covering finite differences. This thesis deals with the central difference approximation. Most texts develop full-station central difference, however, very little is written on the use of half-stations. This section presents a comparison between half- and full-station central difference, while also indicating the basic steps for coupling the finite difference method with plate buckling. A new trigonometric approach is compared to the standard polynomial central difference approximation, and a plate grid system is developed to show how boundary conditions have been incorporated.

Basic Approach

Plate buckling, as considered in this thesis, makes use of the central finite difference method. The following steps indicate how the method was basically employed in the analysis.

1. Discrete grid points were selected to approximate the governing partial differential equation within

the plate.

2. The central finite difference approximation was applied at each grid and/or reference point.
3. Each partial differential equation was reduced to linear algebraic form.
4. The resulting equations were then solved and buckling coefficient determined.

Half-Station versus Full-Station

For the derivation of finite difference expressions, it is necessary to work with grid arrangements. Finite difference grids for a one-dimensional case are shown in Figure 3.1 and Figure 3.2. Grid points (indicated by circles) represent discretely defined functional values while reference points, indicated by an x in Figure 3.2, locate the position of the functional value desired. Grid points can be coincident with reference points but this is not mandatory. The degrees of freedom of the system are the specific values of the unknown functions located at grid points. The spacing between mesh lines was held constant. The grid lines in x- and y- directions are represented by the symbols h_x and h_y respectively.

To develop half-station central difference equations, in which the reference point is located between grid points, one can evaluate a function g , at point R_j (Fig 3.2) using a Taylor series expansion. This of course, implies continuity

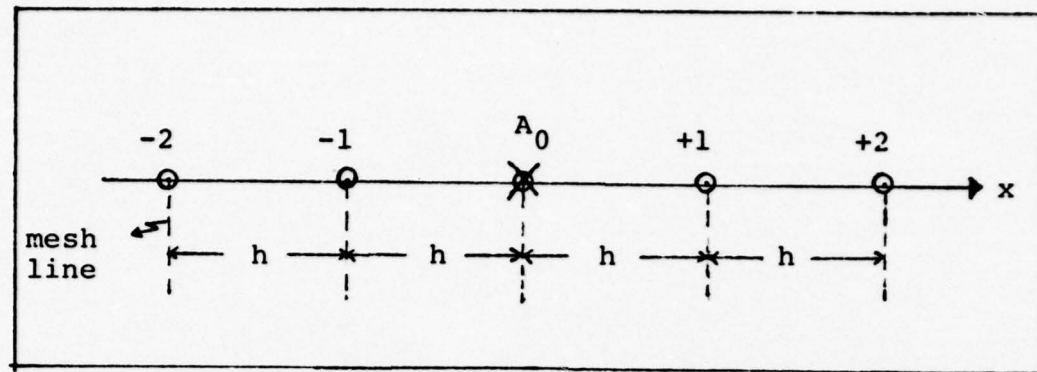


Figure 3.1 Finite Difference Grid

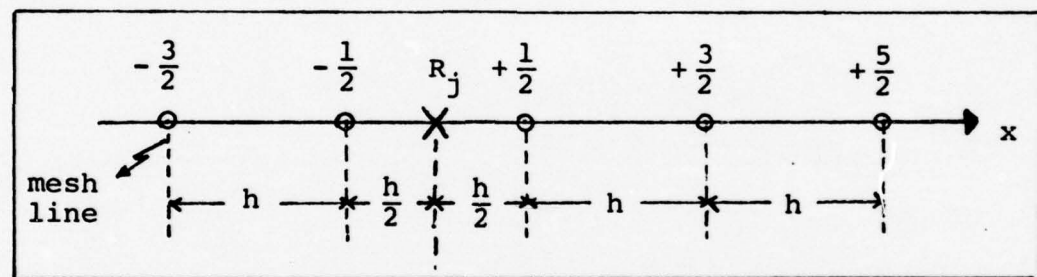


Figure 3.2 Half-station Finite Difference Grid

conditions for each functional relationship. The basic Taylor series can be stated as

$$g_{(at -3/2)} = (g + \alpha_{ij} g' + \frac{1}{2!} \alpha_{ij}^2 g'' + \frac{1}{3!} \alpha_{ij}^3 g''' + \dots) \text{ (at } R_j \text{)} \quad (3-1)$$

where primes denote order of derivatives and

$$\alpha_{ij} = (x_{at -3/2} - x_{at R_j}) \quad (3-2)$$

and $\alpha_{ij} = h$ (a constant mesh size). It is now possible to incorporate the above expressions for specific locations.

$$g_{-3/2} = g - \frac{3h}{2} g' + \frac{1}{2} \left(\frac{3h}{2}\right)^2 g'' - \frac{1}{6} \left(\frac{3h}{2}\right)^3 g''' + \frac{1}{24} \left(\frac{3h}{2}\right)^4 g^{iv} - \dots \quad (3-3)$$

$$g_{-1/2} = g - \frac{h}{2} g' + \frac{1}{2} \left(\frac{h}{2}\right)^2 g'' - \frac{1}{6} \left(\frac{h}{2}\right)^3 g''' + \frac{1}{24} \left(\frac{h}{2}\right)^4 g^{iv} - \dots \quad (3-4)$$

$$g_{+1/2} = g + \frac{h}{2} g' + \frac{1}{2} \left(\frac{h}{2}\right)^2 g'' + \frac{1}{6} \left(\frac{h}{2}\right)^3 g''' + \frac{1}{24} \left(\frac{h}{2}\right)^4 g^{iv} + \dots \quad (3-5)$$

$$g_{+3/2} = g + \frac{3h}{2} g' + \frac{1}{2} \left(\frac{3h}{2}\right)^2 g'' + \frac{1}{6} \left(\frac{3h}{2}\right)^3 g''' + \frac{1}{24} \left(\frac{3h}{2}\right)^4 g^{iv} + \dots \quad (3-6)$$

Equation (3-4) is subtracted from equation (3-5) yielding

$$g' = \frac{1}{h} (g_{+1/2} - g_{-1/2}) - \frac{h^2}{24} g''' \quad (3-7)$$

where the half-station representation of the first derivative is

$$g' = \frac{1}{h} (g_{+1/2} - g_{-1/2}) \quad (3-8)$$

and $\frac{h^2}{24} g'''$ represents the error approximation [5]. On the other hand, if equations (3-4) and (3-3) are added to equations (3-5) and 3-6), respectively, one obtains the following expressions

$$g_{+1/2} + g_{-1/2} = 2g + \left(\frac{h}{2}\right)^2 g'' + \frac{1}{12} \left(\frac{h}{2}\right)^4 g^{iv} \quad (3-9)$$

$$g_{+3/2} + g_{-3/2} = 2g + \left(\frac{3h}{2}\right)^2 g'' + \frac{1}{12} \left(\frac{3h}{2}\right)^4 g^{iv} \quad (3-10)$$

One can solve equation (3-9) for $2g$ and substitute into equation (3-10)

$$g_{+3/2} - g_{+1/2} - g_{-1/2} + g_{-3/2} = 2h^2 g'' + \frac{5h^4}{12} g^{iv} \quad (3-11)$$

This last equation yields the second derivative based upon half-stations

$$g'' = \frac{1}{2h^2} (g_{+3/2} - g_{+1/2} - g_{-1/2} + g_{-3/2}) - \frac{5h^2}{24} g^{iv} \quad (3-12)$$

Thus, using half-station central difference for the first and second derivatives and removing higher order terms, one arrives at

$$g' = \frac{1}{h} (g_{+1/2} - g_{-1/2}) \quad (3-13)$$

$$g'' = \frac{1}{2h^2} (g_{+3/2} - g_{+1/2} - g_{-1/2} + g_{-3/2}) \quad (3-14)$$

Full-station central difference developed in Ref [5] is stated here for completeness.

$$g' = \frac{1}{2h} (g_{+1} - g_{-1}) - \frac{h^2}{6} g''' \quad (3-15)$$

$$g'' = \frac{1}{h^2} (g_{+1} - 2g_0 + g_{-1}) - \frac{h^2}{12} g^{iv} \quad (3-16)$$

It becomes apparent that first order derivatives are best approximated between grid points (half-station) comparing bound error $\frac{h^2}{24} g'''$ versus $\frac{h^2}{6} g'''$ yet, second derivatives can be more accurately determined at the grid points (full-station) if the higher order terms become a consideration $\left[\frac{h^2}{12} g^{iv} \text{ versus } \frac{5h^2}{24} g^{iv} \right]$.

Trigonometric versus Polynomial

The simplest method of obtaining approximate expressions for derivatives of a function $g(x)$ employs the substitution of a parabola. The parabola passes through three specific functional points, Figure 3.3.

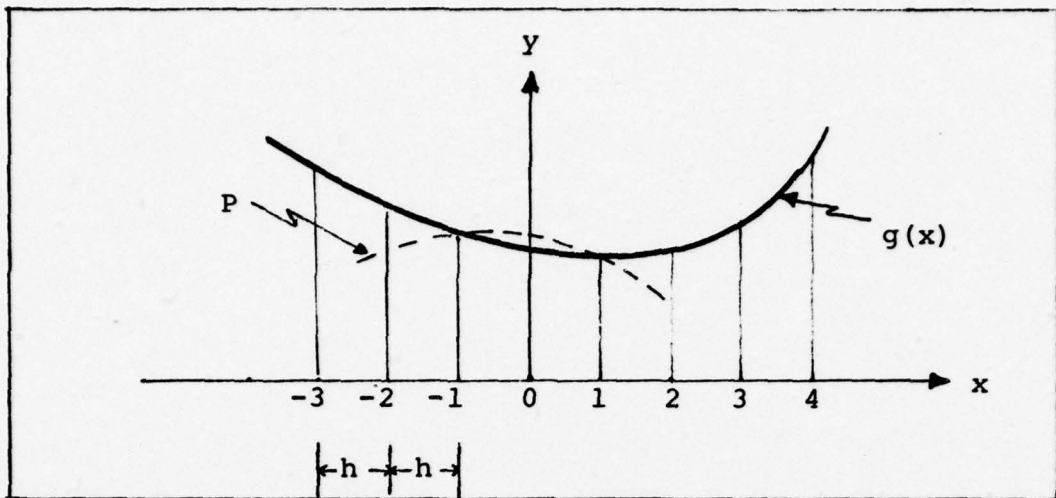


Figure 3.3 Function $g(x)$ and a parabola P

Therefore, one can let $g(x)=P$ where

$$P = Ax^2 + Bx + C \quad (3-17)$$

A , B , and C are constants. Now, evaluate (3-17) at points h , o , and $-h$, respectively.

$$g(h) = Ah^2 + Bh + C = g_{+1} \quad (3-18)$$

$$g(o) = C = g_o \quad (3-19)$$

$$g(-h) = Ah^2 - Bh + C = g_{-1} \quad (3-20)$$

where g_{+1} etc. are in terms of full station central difference notation.

Add equations (3-18) and (3-20)

$$g_{+1} + g_{-1} = 2Ah^2 + 2C \quad (3-21)$$

Next subtract 2 times equation (3-19)

$$2Ah^2 = g_{+1} - 2g_o + g_{-1} \quad (3-22)$$

and rearrange

$$2A = \frac{1}{h^2} [g_{+1} - 2g_o + g_{-1}] \quad (3-23)$$

where the right-hand side of equation (3-23) is the definition of the second-order full station central difference (3-16). One can now take the second derivative (D^2) of equation (3-17) with respect to x .

$$D^2 g(x) = 2A \quad (3-24)$$

Thus, equation (3-24) equals equation (3-23) showing

$$D^2 g(x) = \frac{1}{h^2} [g_{+1} - 2g_0 + g_{-1}] \quad (3-25)$$

Consequently, for this second order system the polynomial approximation of equation (3-17) becomes an equality.

Conventionally the polynomial approximation was used with the central difference technique. However, in 1975 M. Stein and J. Housner [1] decided to let the function $g(x)$ be determined by a trigonometric expression (since the buckling mode shape is normally trigonometric in nature) and they developed a trigonometric finite-difference solution to gain a faster convergence rate. Equation (3-26) allows $g(x)$ to be approximated by a trigonometric expression.

$$g(x) = T_1 + T_2 \sin \frac{\pi(x-x_0)}{\lambda_x} + T_3 \cos \frac{\pi(x-x_0)}{\lambda_x} \quad (3-26)$$

The symbol λ_x represents a wavelength parameter [1].

Earlier paragraphs showed the first derivative could be found by half-station central difference, as

$$Dg(x) = \frac{1}{h} (g_{+1/2} - g_{-1/2}) \quad (3-27)$$

Through the use of equation (3-26) the formation of an equality can be determined as follows

$$Dg(x_o) = \frac{1}{h} \left[g_{+1/2} - g_{-1/2} \right] \quad (3-28)$$

where

$$\frac{1}{h} = \frac{\pi}{2\lambda_x \sin \left[\frac{\pi h}{2\lambda_x} \right]} \quad (3-29)$$

Equation (3-26) is repeated for convenience and its development is indicated in a step-by-step fashion.

$$g(x) = T_1 + T_2 \sin \frac{\pi(x-x_o)}{\lambda_x} + T_3 \cos \frac{\pi(x-x_o)}{\lambda_x} \quad (3-26)$$

1. Take derivative of equation (3-26) with respect to x.

$$Dg(x) = T_2 \frac{\pi}{\lambda_x} \cos \frac{\pi(x-x_o)}{\lambda_x} - T_3 \frac{\pi}{\lambda_x} \sin \frac{\pi(x-x_o)}{\lambda_x} \quad (3-30)$$

2. Evaluate equation (3-30) at $x=x_o$.

$$Dg(x_o) = T_2 \frac{\pi}{\lambda_x} \quad (3-31)$$

where

$$T_2 = \lambda_x Dg(x_o) / \pi \quad (3-32)$$

3. Now evaluate equation (3-26) at $x_o \pm \frac{h}{2}$

$$\begin{aligned} g_{+1/2} &= T_1 + T_2 \sin \frac{\pi}{\lambda_x} \left[x_o + \frac{h}{2} - x_o \right] \\ &+ T_3 \cos \frac{\pi}{\lambda_x} \left[x_o + \frac{h}{2} - x_o \right] \end{aligned} \quad (3-33)$$

$$g_{+1/2} = T_1 + T_2 \sin \frac{\pi h}{2\lambda_x} + T_3 \cos \frac{\pi h}{2\lambda_x} \quad (3-34)$$

$$g_{-1/2} = T_1 + T_2 \sin \left[-\frac{\pi h}{2\lambda_x} \right] + T_3 \cos \left[-\frac{\pi h}{2\lambda_x} \right] \quad (3-35)$$

NOTE: $\cos(-u) = \cos u$ and $\sin(-u) = -\sin u$

4. Subtract equation (3-35) from (3-33).

$$g_{+1/2} - g_{-1/2} = 2T_2 \sin \frac{\pi h}{2\lambda_x} \quad (3-36)$$

5. Equation (3-32) is substituted.

$$g_{+1/2} - g_{-1/2} = \frac{2\lambda_x}{\pi} Dg(x_o) \sin \frac{\pi h}{2\lambda_x} \quad (3-37)$$

6. Rearrange equation (3-37).

$$Dg(x_o) = \frac{\pi}{2\lambda_x \sin \frac{\pi h}{2\lambda_x}} [g_{+1/2} - g_{-1/2}] \quad (3-38)$$

or

$$Dg(x_o) = \frac{1}{h} [g_{+1/2} - g_{-1/2}] \quad (3-38a)$$

The reader can observe in equation (3-38) that as the wavelength λ_x approaches infinity, h approached h , since the $\sin(\pi h/2\lambda_x)$ approached $(\pi h/2\lambda_x)$, thus reducing the trigonometric expression to the conventional difference expression.

Both trigonometric and polynomial finite difference are used to approximate the virtual work equation.

Mesh Arrangement in the Virtual Work Equation

In order to acquaint the reader more fully with the use of half-station for first order partial derivatives and full-station for second order partials an example follows, employing the trigonometric technique. The virtual work equation (2-6) is repeated here for completeness.

$$\int_0^b \int_0^a (M_x \delta w_{xx} + M_y \delta w_{yy} + 2M_{xy} \delta w_{xy}) dx dy = \int_0^a \int_0^b (N_x w_{x,x} \delta w_{x,x}) dy dx \quad (2-6)$$

Partial derivatives are replaced by the following trigometric central difference expressions

$$\begin{aligned} (w_{xx})_{i,j} &= (w_{i+1,j} - 2w_{ij} + w_{i-1,j})/\hat{h}_x^2 \\ (w_{yy})_{i,j} &= (w_{i,j+1} - 2w_{ij} + w_{i,j-1})/\hat{h}_y^2 \quad (3-39) \\ (w_{xy})_{ij} &= (w_{i+1,j+1} - w_{i,j+1} - w_{i+1,j} + w_{ij})/\hat{h}_x\hat{h}_y \end{aligned}$$

where \hat{h}_x and \hat{h}_y have been defined in equation (3-29).

Equation (2-6) can now be stated as

$$\begin{aligned} \delta U = h_x h_y \sum_{j=1}^N \sum_{i=1}^M & \left[\xi_{x_i} \xi_{y_j} \left[D_{11}(w_{i+1,j} - 2w_{ij} \right. \right. \\ & \left. \left. + w_{i-1,j})/\hat{h}_x^4 + D_{12}(w_{i,j+1} - 2w_{ij} + w_{i,j-1})/ \right. \right. \\ & \left. \left. \hat{h}_x^2 \hat{h}_y^2 \right] \left[\delta w_{i+1,j} - 2\delta w_{ij} + \delta w_{i-1,j} \right] \right. \\ & \left. + \xi_{x_i} \xi_{y_j} \left[D_{12}(w_{i+1,j} - 2w_{ij} + w_{i-1,j})/\hat{h}_y^2 \hat{h}_x^2 \right. \right. \\ & \left. \left. + D_{22}(w_{i,j+1} - 2w_{ij} + w_{i,j-1})/\hat{h}_y^4 \right] \left[\delta w_{i,j+1} \right. \right. \\ & \left. \left. - 2\delta w_{ij} + \delta w_{i,j-1} \right] + 2n_{x_i} n_{y_j} \left[2D_{66}(w_{i+1,j+1} \right. \right. \\ & \left. \left. - w_{i,j+1} - w_{i+1,j} + w_{ij})(\delta w_{i+1,j+1} - \delta w_{i,j+1} \right. \right. \\ & \left. \left. - \delta w_{i+1,j} + \delta w_{ij})/\hat{h}_x^2 \hat{h}_y^2 \right] \right] \quad (3-40) \end{aligned}$$

where integers N and M are the total number of finite difference stations in the x- and y- directions and the ξ and n coefficients equal

$$\begin{aligned}\xi_{xi} &= 0 \text{ when } i < I_1 \text{ or } i > I_3 \\ &= 1/2 \text{ when } i = I_1 \text{ or } i = I_3\end{aligned}\quad (3-41)$$

$$= 1 \text{ when } I_1 < i < I_3$$

$$\begin{aligned}\xi_{xj} &= 0 \text{ when } j < J_4 \text{ or } j > J_4 \\ &= 1/2 \text{ when } j = J_4 \text{ or } j = J_2\end{aligned}\quad (3-42)$$

$$= 1 \text{ when } J_4 < j < J_2$$

$$\begin{aligned}n_{xi} &= 0 \text{ when } i < I_1 \text{ or } i \geq I_3 \\ &= 1 \text{ when } I_1 \leq i < I_3\end{aligned}\quad (3-43)$$

$$\begin{aligned}n_{yj} &= 0 \text{ when } j < J_4 \text{ or } j \geq J_2 \\ &= 1 \text{ when } J_4 \leq j < J_2\end{aligned}\quad (3-44)$$

I_1 and I_3 designate the grid row of boundaries 1 and 3 while J_2 and J_4 are column designators for boundaries 2 and 4 (Fig. 3.4). The right hand side of equation (2-6) can also be expanded incorporating

$$w_{,x} = (w_{i+1,j} - w_{ij})/\hat{h}_x \quad (3-45)$$

$$w_{,y} = (w_{i,j+1} - w_{ij})/\hat{h}_y \quad (3-46)$$

$$\begin{aligned}w_{,y} \delta w_{,x} &= (w_{i,j+1} - w_{ij} + w_{i+1,j+1} - w_{i+1,j})(\delta w_{i+1,j} \\ &\quad - \delta w_{ij} + \delta w_{i+1,j+1} - \delta w_{i,j+1})/4\hat{h}_x \hat{h}_y\end{aligned}\quad (3-47)$$

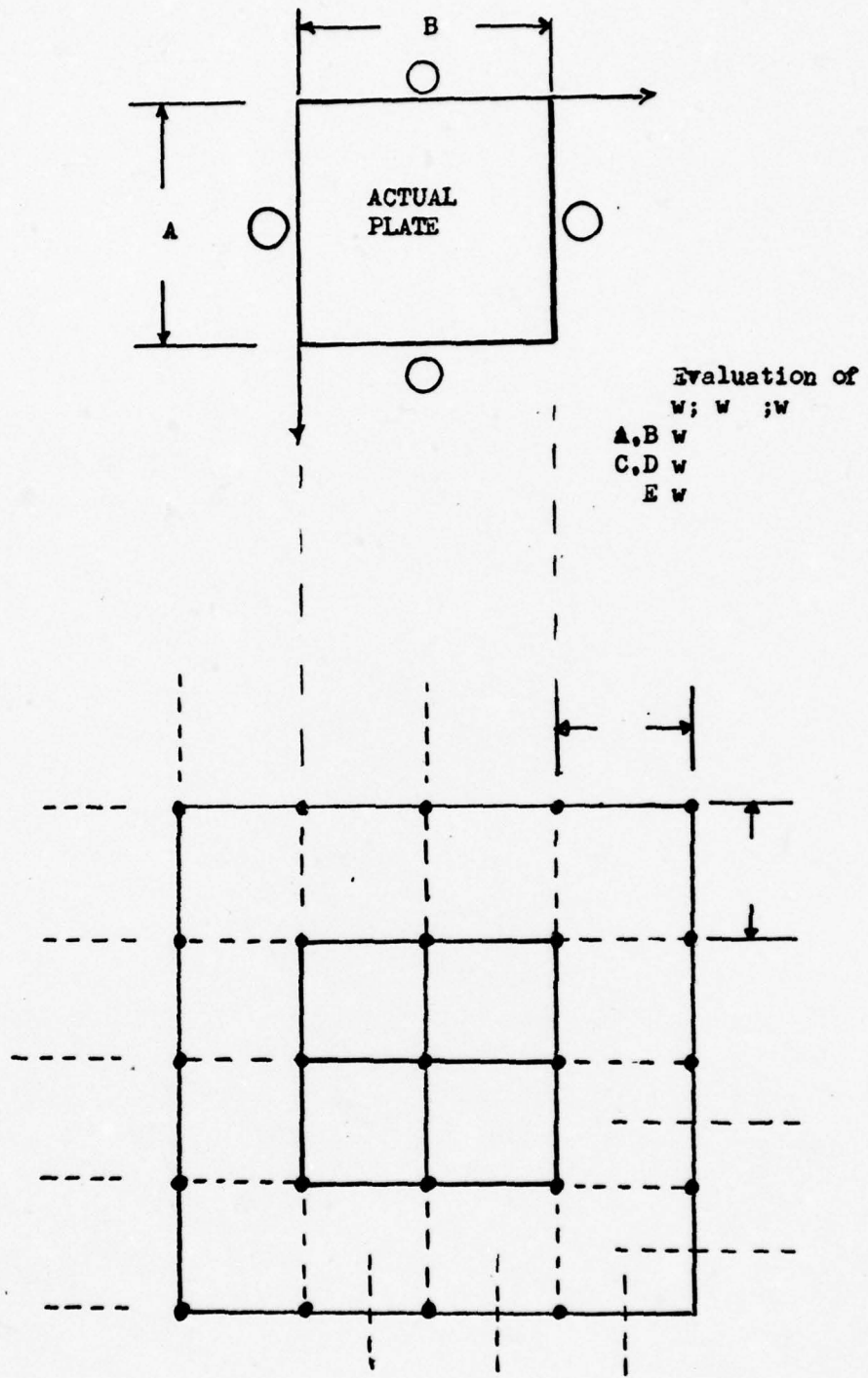


Figure 3.4 Grid Arrangement

and a similar arrangement for $w_{,x} \delta w_{,x}$. To fully appreciate the development of the above equations, the reader's attention is directed to grid point 7 of a twenty-five degree grid arrangement in Figure 3.4. The numerical approximation $w_{,x}$ and its variation $\delta w_{,x}$ are evaluated at reference point A using half-station central difference. Thus grid point 12 is incorporated with grid point 7.

$$w_{,x} \delta w_{,x} = (w_{12} - w_7)(\delta w_{12} - \delta w_7)/\hat{h}_x^2 \quad (3-48)$$

The same procedure is applied to $w_{,y} \delta w_{,y}$ in the y-direction. A problem occurs when two different directional derivatives (i.e. $w_{,y} \delta w_{,x}$) become involved. This is due to the fact that derivative functions must be incorporated into the volume integral using constant quantities ($h_x h_y (\xi_{x_i} \xi_{y_j})$).

In the case referred to above separate ordinate values (L and M) would be obtained at reference points A and C (Figure 3.5), respectively

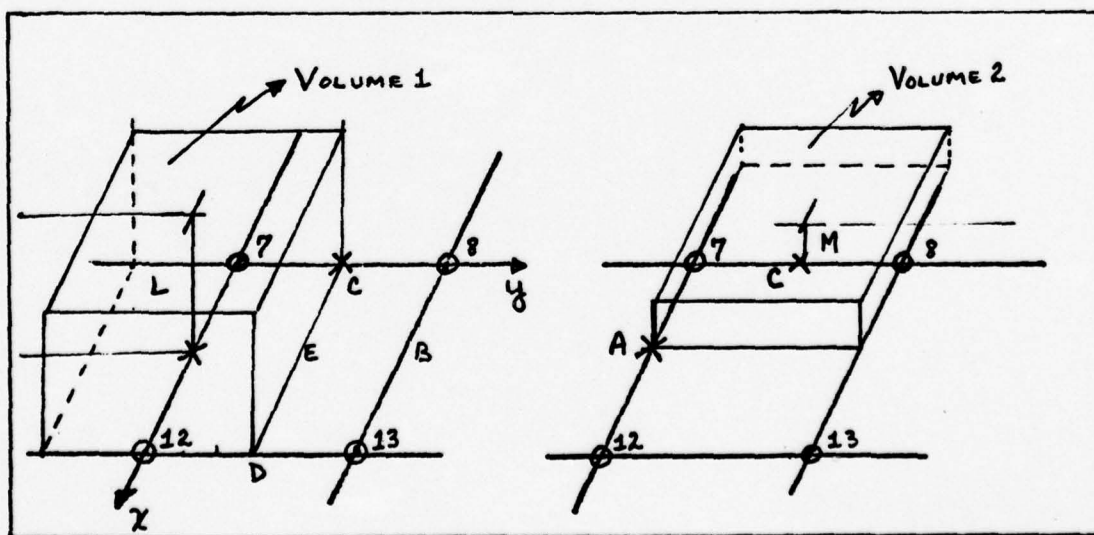


Figure 3.5 Half-Station Differences of $w_{,y}$ and $\delta w_{,x}$.

Consequently, two ordinate values are obtained, but they are associated with two distinct volumes for the same functional $w_{,x} \delta w_{,y}$. In order to maintain a half-station technique and to associate the product of two separate directional derivatives with a particular volume, a reference point is located at position E and is evaluated in the following manner.

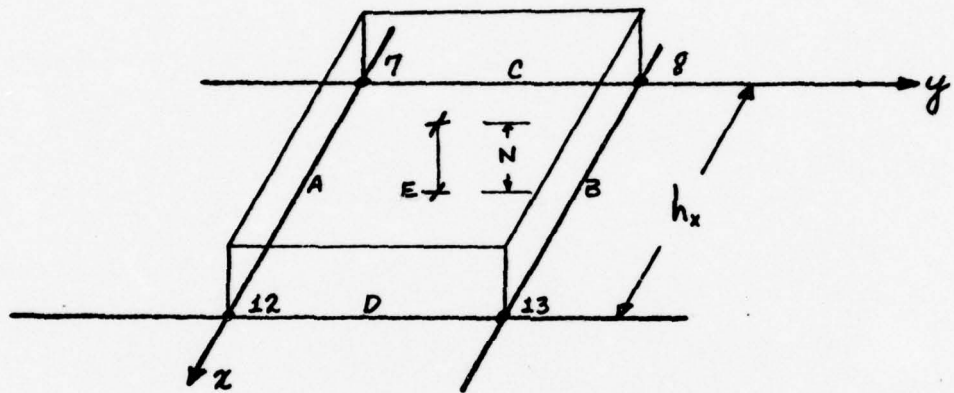


Figure 3.6 The Position of a Reference Point to Evaluate a Mixed Derivative.

The half-station central difference of point E is

$$w_{,y} = (w_B - w_A) / \hat{h}_y \quad (3-49)$$

where $w_B = (w_{13} + w_8)/2$ and $w_A = (w_{12} + w_7)/2$

$$\delta w_{,x} = (\delta w_D - \delta w_C) / \hat{h}_x \quad (3-50)$$

where $\delta w_D = (\delta w_{13} + \delta w_{12})/2$ and $\delta w_C = (\delta w_8 + \delta w_7)/2$

therefore

$$\begin{aligned} w_{,y} \delta w_{,x} &= (w_8 - w_7 + w_{13} - w_{12}) / (\delta w_{12} \\ &\quad - \delta w_7 + \delta w_{13} - \delta w_8) / 4 \hat{h}_x \hat{h}_y \end{aligned} \quad (3-51)$$

thus in total agreement with general form of Equation (3-47).

Mention has been made of volume referenced to a particular derivative approximation. The volume is defined as the area $h_x h_y$ times the ordinate value at a given grid/reference point. By treating the volume as a parallelopiped, errors are developed in the total integral since step function expressions are created with respect to grid arrangement. The effects are more noticeable at larger mesh size (lower number of degrees of freedom).

The above paragraphs have shown how the finite difference approximations replace the partial derivatives within a virtual work expression, now the steps leading to the final buckling equation are discussed. The first step is to factor all common expressions that relate to specific δw_{ij} 's. Thus

$$\sum_{i=1}^M \sum_{j=1}^N (C_{ij} + A_{ij} N_x) \delta w_{ij} = 0 \quad (3-52)$$

where N_x is the only externally applied force considered.

And

$$C_{ij} = \xi_{y_j} \frac{1}{\hat{h}_x^2} \left[\xi_{x_{i+1}} M_{x_{i+1,j}} - 2 \xi_{x_i} M_{x_{ij}} \right. \\ \left. + \xi_{x_{i-1}} M_{x_{i-1,j}} \right] + \xi_{x_i} \frac{1}{\hat{h}_y^2} \left[\xi_{y_{j+1}} M_{y_{i,j+1}} \right. \\ \left. - 2 \xi_{y_j} M_{y_{ij}} + \xi_{y_{j-1}} M_{y_{i,j-1}} \right] + \frac{1}{\hat{h}_x \hat{h}_y} \\ \left[n_{x_{i-1}} n_{y_{j-1}} M_{xy_{i-1,j-1}} - n_{x_{i-1}} n_{y_j} M_{xy_{i-1,j}} \right. \\ \left. - n_{x_i} n_{y_{j-1}} M_{xy_{i,j-1}} + n_{x_i} n_{y_j} M_{xy_{ij}} \right] \quad (3-53)$$

$$A_{ij} = \left[\xi_{y_j} n_{y_i} (w_{i+1,j} - w_{ij}) - \xi_{y_j} n_{x_{i-1}} (w_{ij} - w_{i-1,j}) \right] / \hat{h}_x^2 \quad (3-54)$$

The reader is directed to Appendix B for the development of several terms comprising coefficients C_{ij} and A_{ij} . It becomes obvious that in Equation (3-52), the only way a zero result can be obtained is for

$$[C_{ij} + A_{ij} N_x] = 0 \quad (3-55)$$

since δw_{ij} are arbitrary values throughout the domain.

There is a second ordering step required for evaluating a buckling quantity. In Equation (3-55) the displacement terms (w_{ij} 's) occur (as can be observed in Appendix B) indiscriminately. It therefore becomes necessary to factor and order all the w_{ij} 's leading to an eigenvector expression.

$$\begin{vmatrix} E_{ij} & w_{ij} \end{vmatrix} = 0 \quad (3-56)$$

The E_{ij} matrix contains the quantity N_x (in-plane load) which is the eigenvalue. Reference [1] discusses the numerical approach used in the final reorientation of the displacements. This approach is called the marching technique and is developed in Appendix C of Reference [1].

Finite Difference Approximation of the Equilibrium Equation

It has been stated in Sec II Equation (2-4) that the equation for buckling is a fourth order partial differential equation. The form of this equation is restated here for convenience.

$$w_{xxxx} + 2w_{xxxy} + w_{yyyy} = N_x w_{xx} \quad (3-57)$$

The finite difference approximation to this equation is established by making use of full-station approximations which were developed earlier in this section. This difference technique can be found in several references. An excellent reference which presents a detailed example of a plate buckling problem is "Structural Analysis" by Ghali and Neville [26]. Thus for further elaboration on the equilibrium approach the reader is directed to the above reference. Yet, for continuity the finite difference molecule is presented in Figure 3.7.

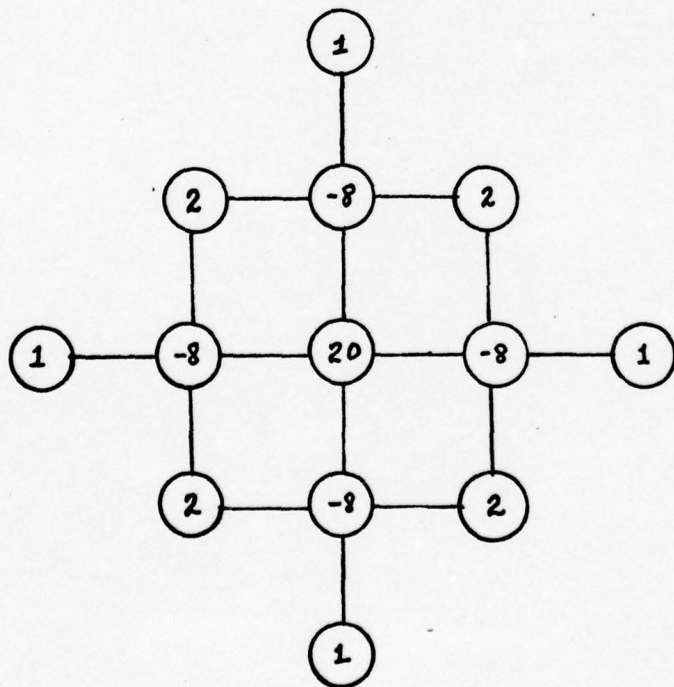


Figure 3.7 Computational Model

IV. Numerical Results

Introduction

Two sets of boundary conditions were investigated. The following terminology is applicable to both the simple support and clamped conditions.

1. Long Plate - This method employs the trigonometric finite difference approximations by choosing the wavelength parameter λ based upon the buckle length of an infinitely long plate [1]. The difference approximations are then substituted into the virtual work equation.
2. Conventional - This method is also used in the virtual work equation and represents the polynomial approach using half- and full-station finite differences.
3. Equilibrium - This label applies to the full-station polynomial finite difference approximations of the equilibrium equation.
4. Lambda - This label represents the values used in the virtual work equation when the buckle wavelength is not based on the buckle length of an infinitely long plate

$$\text{Lambda} = \lambda_x / A \quad (4.1)$$

Values of Lambda are included and discussed to present a broader appreciation of the trigonometric finite difference capabilities.

Throughout this presentation an error of plus or minus five percent is considered acceptable as is normally the case in engineering calculations [27].

Various Aspect Ratios - Simple Support

The long plate theory approach gives accurate findings for simply supported plates under in-plane loading if the aspect ratio (A/B) is an integer (see Fig 4.1). The reader should notice, for fractional ratios, accuracy is affected by assumption of the buckle length equal to the width of the plate. At an aspect ratio of 0.5, the plate under this assumption is more flexible while for a ratio of 1.5, the structure is stiffer. Yet, comparatively speaking, a long plate assumption incorporated into finite difference approximations of the virtual work expression, yields results more favorable than the conventional virtual work or equilibrium equation approach. The last two approaches yield about the same results. One should also notice that increasing the degrees of freedom (D.O.F.) allows a better evaluation of boundary condition effects and hence less error.

Various Aspect Ratios - Clamped

Many of the above statements become appropo for clamped plates (Fig 4.2). Long plate theory gives the best results for mid-range aspect ratios while conventional virtual work and equilibrium results parallel each other. It appears for aspect ratios 1 to 4 at least 81 D.O.F. are needed to keep

accuracy to 5 percent. One notices at an aspect ratio of 0.5 that the results are more favorable than for the rest of the aspect ratios. For this aspect ratio we have a situation in which the boundary conditions are more realistically modeled by the constant mesh arrangement since the plate is acting similar to a wide beam. At higher aspect ratios a constant mesh size doesn't properly credit the influences of the boundary effects. Thus to obtain 5 percent accuracy for a buckling clamped plate one should use at least 81 D.O.F. and refine the mesh size near the boundaries.

Degrees of Freedom versus Error - Simple Support

Aspect Ratio 0.5. This discussion concerns Fig 4.3 and the rectangular plate in this case is similar to a beam where the boundaries, parallel to the in-plane load N_x , are far away from the load itself. In assuming long plate theory the results for low degrees of freedom are very good in fact the comparative curves--equilibrium, conventional and Lambda ($>1.$) give excellent results. In essence, long plate theory makes use of the fact that the buckled length is equal to the width of the plate, this can be illustrated by Fig 4.a.

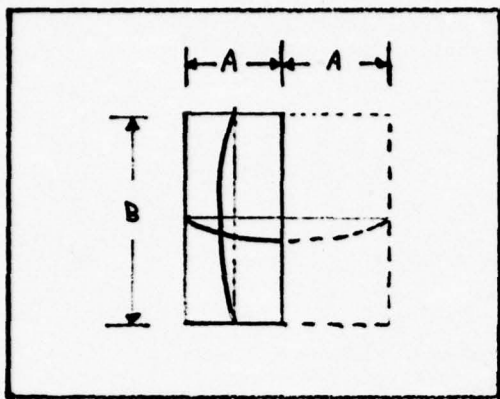


Fig 4.a Long Plate Theory

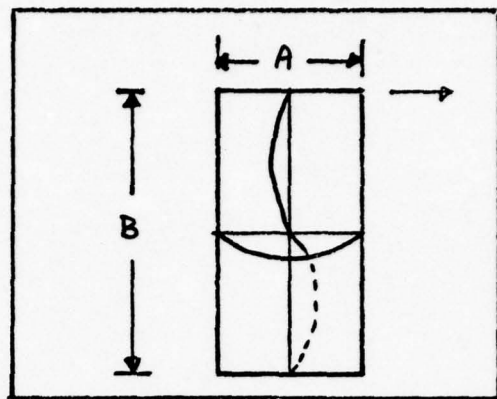


Fig 4.b $\lambda_x/A = 1$

Now when a value of 1 is selected for Lambda (λ_x/A), this assumes a buckle length in the y-direction equal to one-half B (Fig 4.b). This comes from a basic equation (4.2) developed in Reference [1] to calculate the parameters.

$$\frac{\lambda_y}{B} \div \frac{\lambda_x}{A} = \beta. \quad (4-2)$$

β is equal to the aspect ratio for simply supported plates and 1.5 when the plates are clamped [28]. The reason the accuracy isn't as good as long plate theory is that equation (4-2) for Lambda=1 shows the two buckle lengths in the y-direction rather than an ideal 1 half-sine wave for the length. Considering Lambda=0.5, then $\lambda_y/B \div 0.5 = 0.5$ yields $B=4\lambda_y$ thus now there are four buckle lengths in the y-direction and two in the x-direction hence a stiffer plate. This is realistically pointing out what Timoshenko [6] describes graphically (whenever more than one half-sine wave is assumed in the y-direction the plate is stiffer). The curves also indicate a band of Lambda values exist

from one to infinity (Conventional method) that present excellent results at low D.O.F. as do the Equilibrium and Long Plate methods, while for values of Lambda approaching zero, the results become erroneous as the plate becomes stiffer (from a buckling viewpoint).

Aspect Ratio 1.0. Again excellent results at low D.O.F., with the Long Plate method showing no error (Fig 4.4) as was expected since buckle width does equal buckle length. A band of Lambda values greater than or equal to 0.8 provides good results. Aspect ratios 2 and 3 also follow these trends (Figs. 4.5 and 4.6).

Aspect Ratio 5.0. In this instance, the curves (Fig 4.7) have inflection points at lower degrees of freedom. The reader should remember, especially for this set of curves, the concept being incorporated into the analysis by assuming various values of Lambda. In effect, a functional value for the displacement is assumed at buckling in the virtual work approach. The form of the function selected is like that used in the Rayleigh-Ritz technique which, in essence, requires at least the satisfaction of the kinematic boundary conditions for rapid convergence. It becomes apparent that certain Lambda ratios do not provide functions that meet the boundary conditions properly, (see Fig 4.c), thus one can expect greater inaccuracy at lower D.O.F. The Long Plate method, however, gives excellent results at low D.O.F. because the boundary

conditions are satisfied displacement-wise (see Fig 4.d).

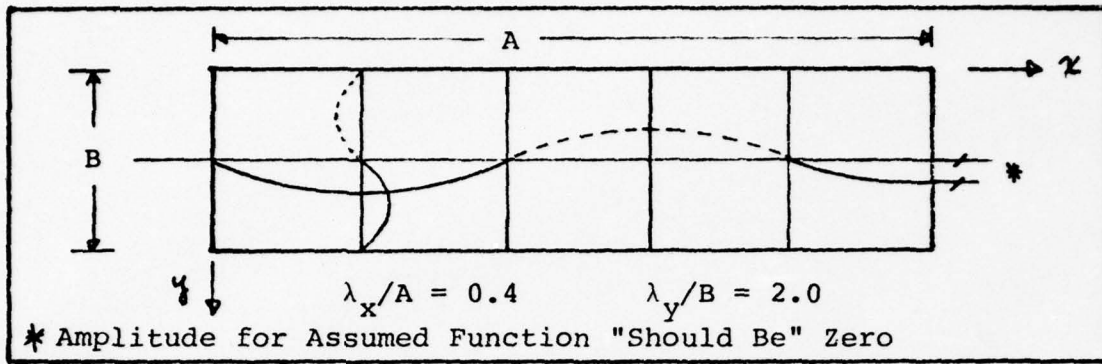


Fig 4.c A Lambda Value Displacement Function.

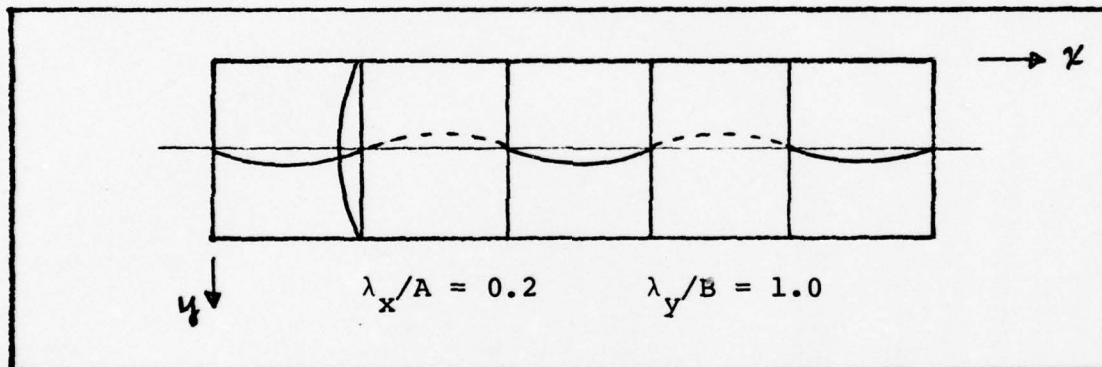


Fig 4.d Long Plate Theory Displacement Function.

At higher D.O.F. (64) all curves present monotonically decreasing error values. This is expected since the assumed function becomes secondary with its inclusion into the virtual work equation.

Degrees of Freedom versus Error - Clamped

Aspect Ratio 0.5. This discussion concerns Fig 4.8. Again we have the conventional virtual work and equilibrium method providing almost identical results while the long plate theory in the trigonometric approximations gives

slightly better results. It is also noticed that a "good" selection of Lambda (0.65) produces better results at low D.O.F. This is expected and explained by the fundamental assumption of Long Plate Theory where the width equals the buckle length. In reality, however, the clamped boundary prohibits a full half-sine wave (see Fig 4.e). Thus, with $\Lambda = 0.65$, $\lambda_y = .975b$ which is more realistic. Aspect 1 and 2 present the same tendencies, only higher D.O.F. are needed for better accuracy.

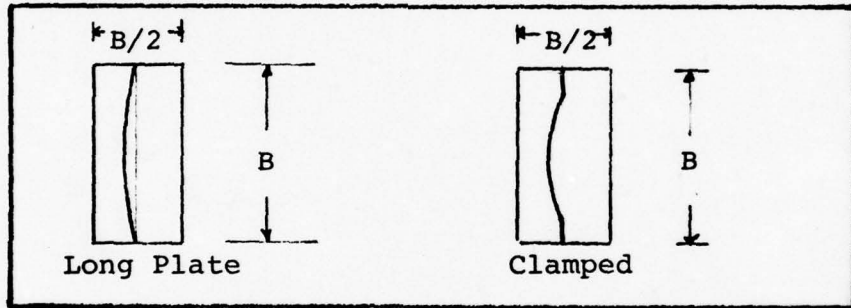


Fig 4.e Assumption Versus Actual Wavelength in a Clamped Plate.

Aspect Ratio 3.0. Concerning the interpretation of the Lambda band, the relative closeness of the Conventional and Equilibrium methods, and the ability of the trigonometric finite difference method employing Long Plate theory to be slightly better than the Conventional and Equilibrium methods, (Fig 4.11) one can use the previously stated observations. Inflection points again occur at low degrees of freedom showing a tendency to be oscillatory. An explanation of this phenomenon was previously presented. One can observe that even with the conventional approach,

potential energy wise, it's more accurate to select 25 D.O.F. versus 36. This peculiarity is attributed to the failure of the selected function to appropriately consider the boundary conditions. Salvadori [29] in analyzing equilibrium methods experienced oscillations similar to these for certain cases. It should be noted by the reader that when inflection points do occur, long plate curves are not effected. This was true in the simple support case (Fig 4.7) and also is true in the clamped cases (Fig 4.11 and 4.12). The assumption of buckle width equal to the width of the plate seems to incorporate boundary conditions more accurately (like the simple support cases). This again indicates that the inflection point is probably being caused by poor approximation of boundary conditions at low D.O.F. as well as an insufficient number of node points adjacent to the boundary which was previously pointed out.

Aspect Ratio 5.0. Oscillation is now apparent and troublesome for all curves (except long plate) in Fig 4.12. Higher D.O.F. are needed to maintain accuracy and this is expected since again we have increased the mesh size at low D.O.F. and the finite difference approximations don't represent the boundaries accurately. Previous Lambda interpretations are still consistent for this long clamped plate as well as the close proximity of the conventional and equilibrium curves. The value of the trigonometric approach can be appreciated here when it is apparent a

Lambda value of 0.10 would have given accurate results around 64 D.O.F. compared to 81 or higher for all other selections.

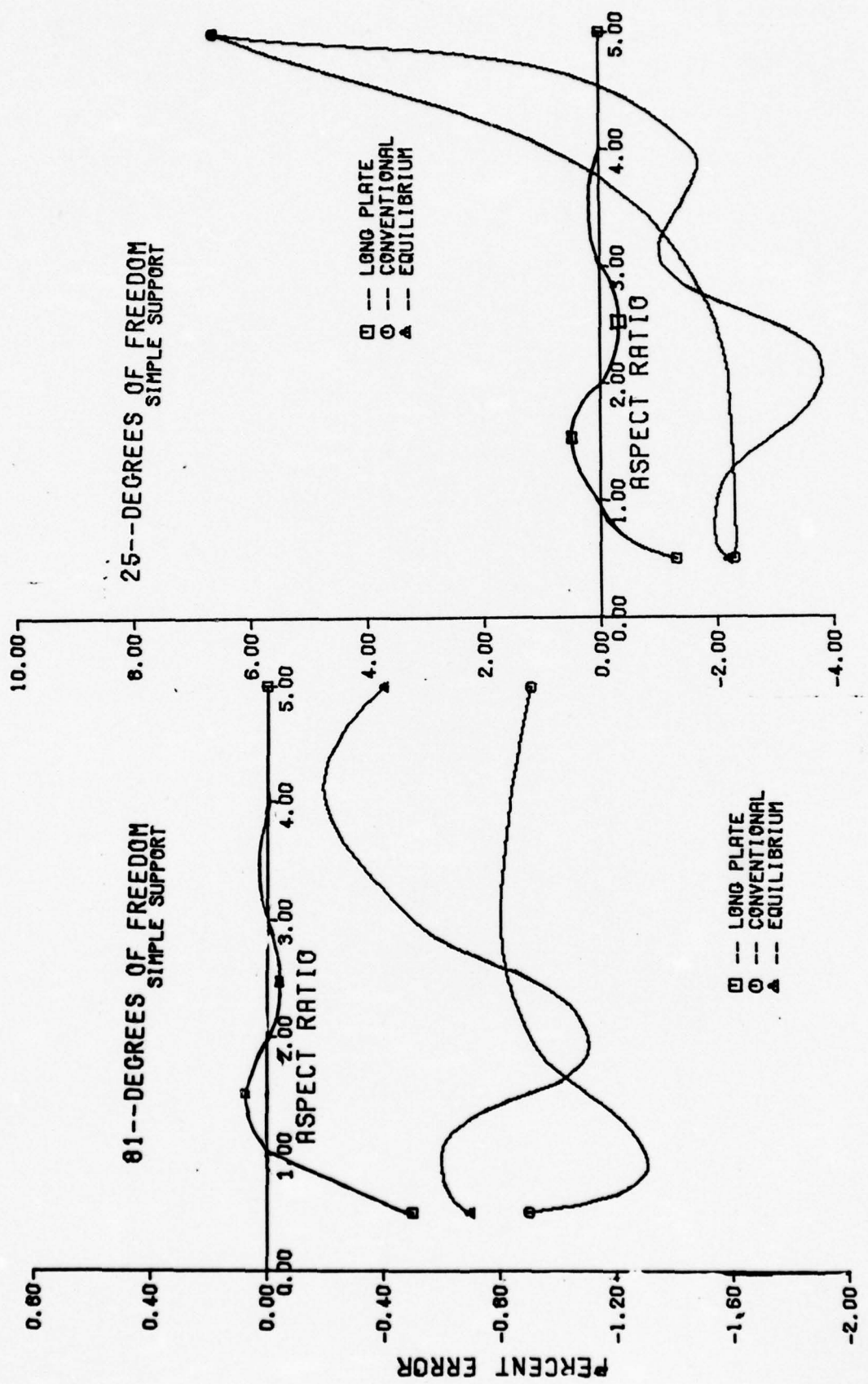


FIGURE 4.1 FINITE DIFFERENCE APPROXIMATIONS

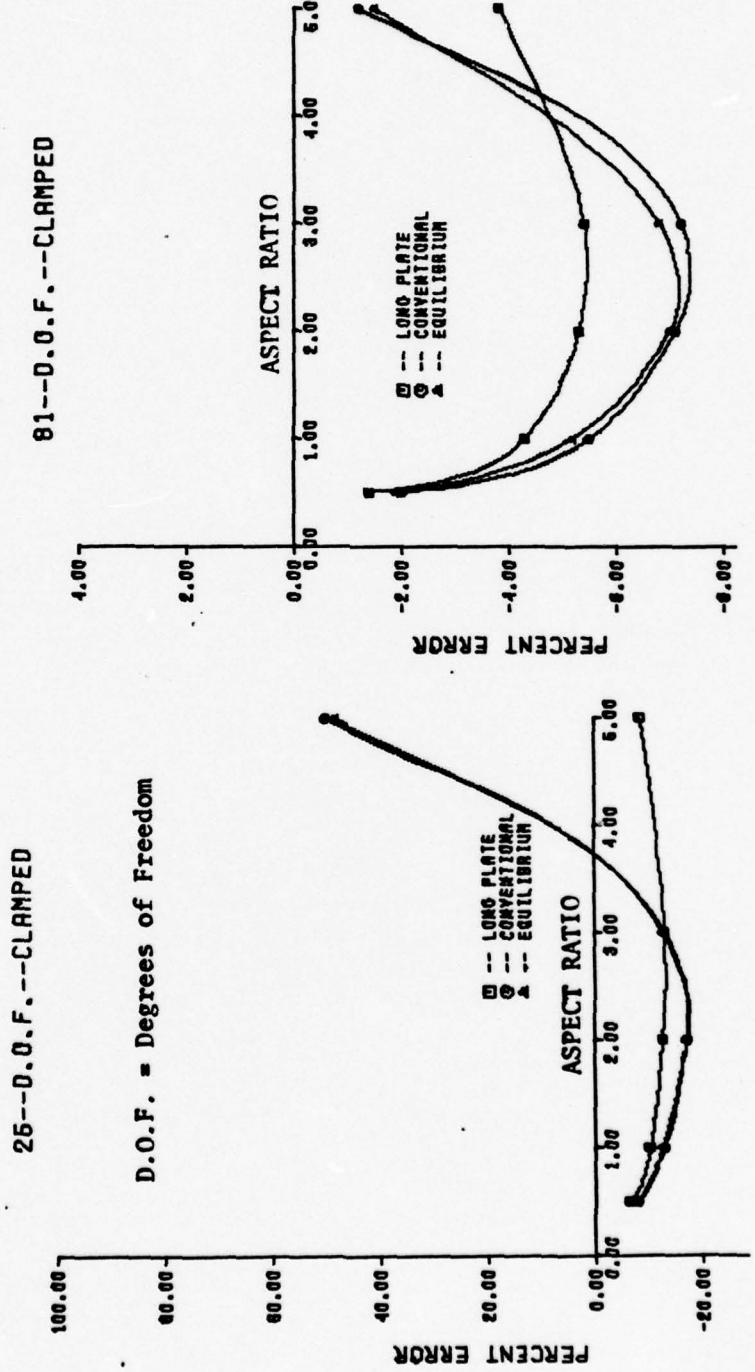


FIGURE 4.2 FINITE DIFFERENCE APPROXIMATIONS

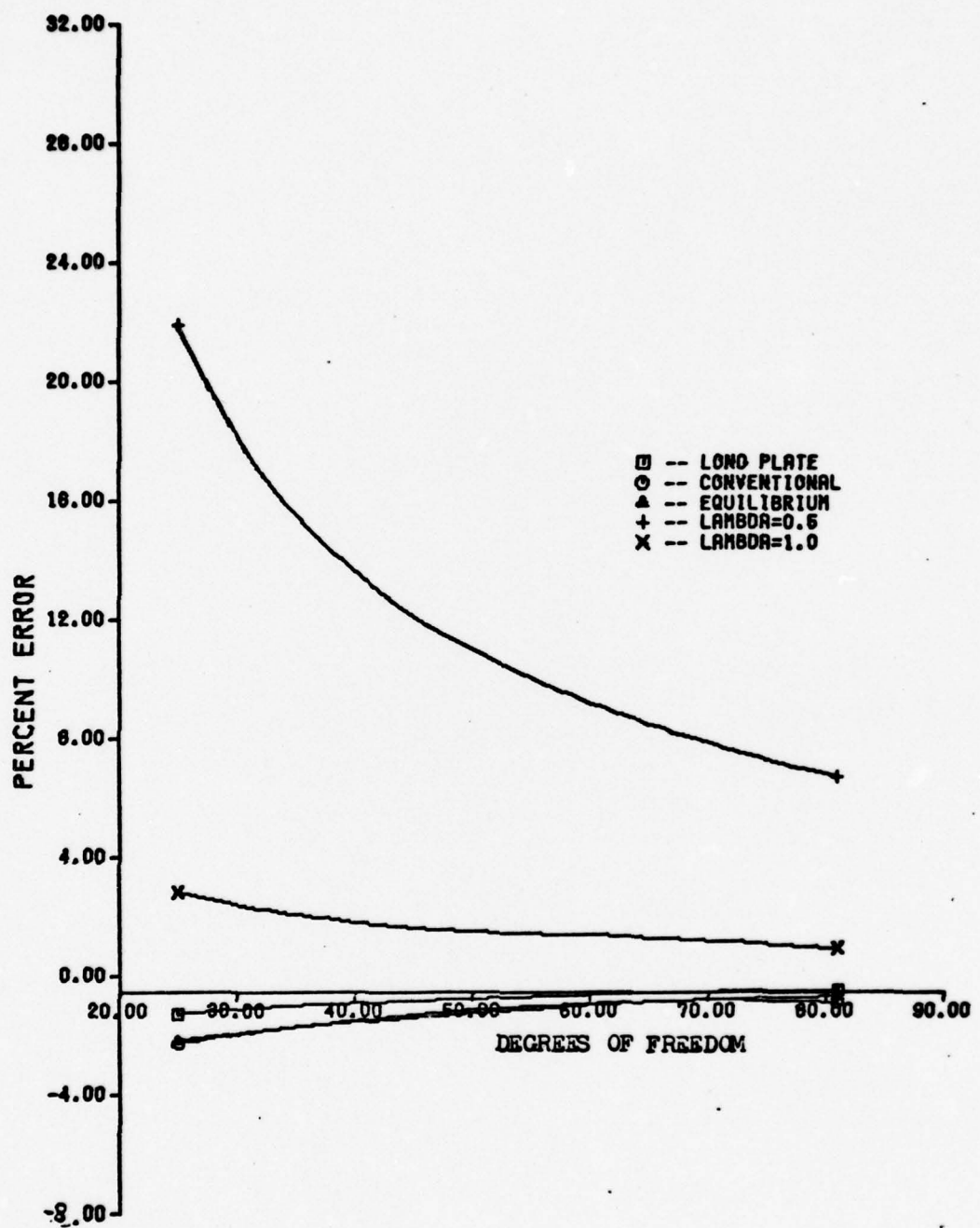


FIGURE 4.3 SIMPLE SUPPORTED PLATE $A/B=0.5$.

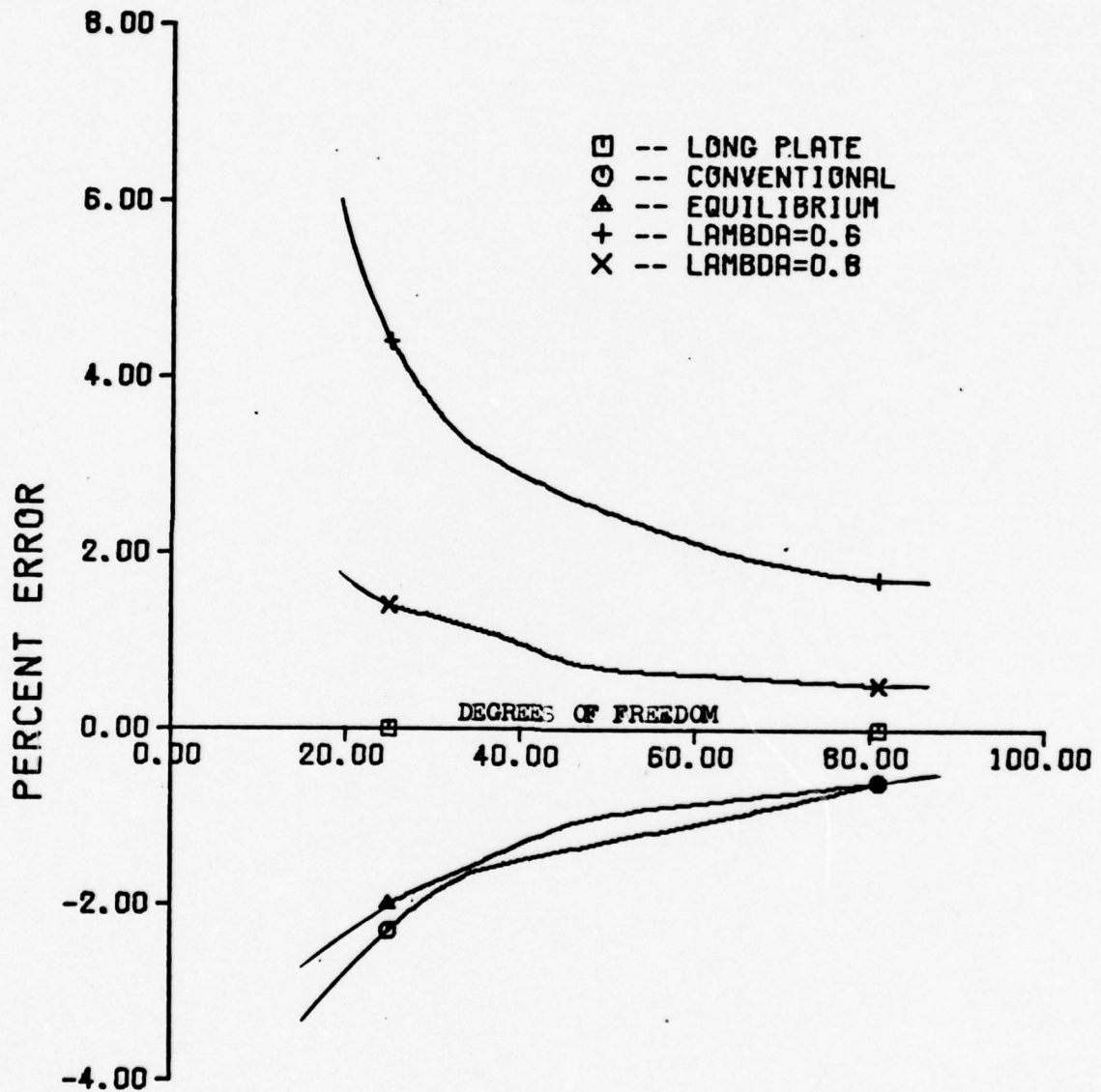


FIGURE 4.4 SIMPLE SUPPORTED PLATE $A/B=1.0$.

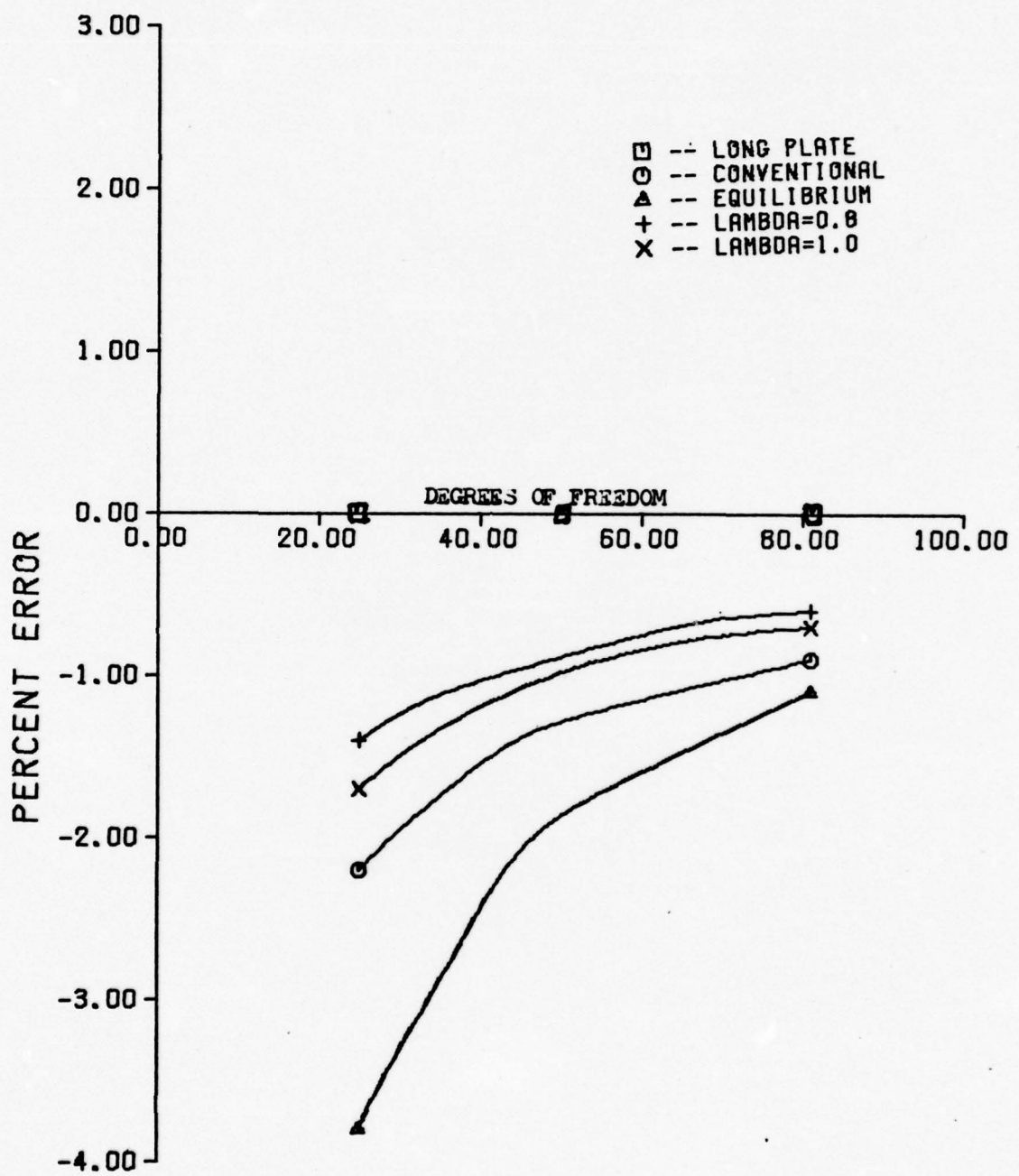


FIGURE 4.5 SIMPLE SUPPORTED PLATE $A/B=2.0$.

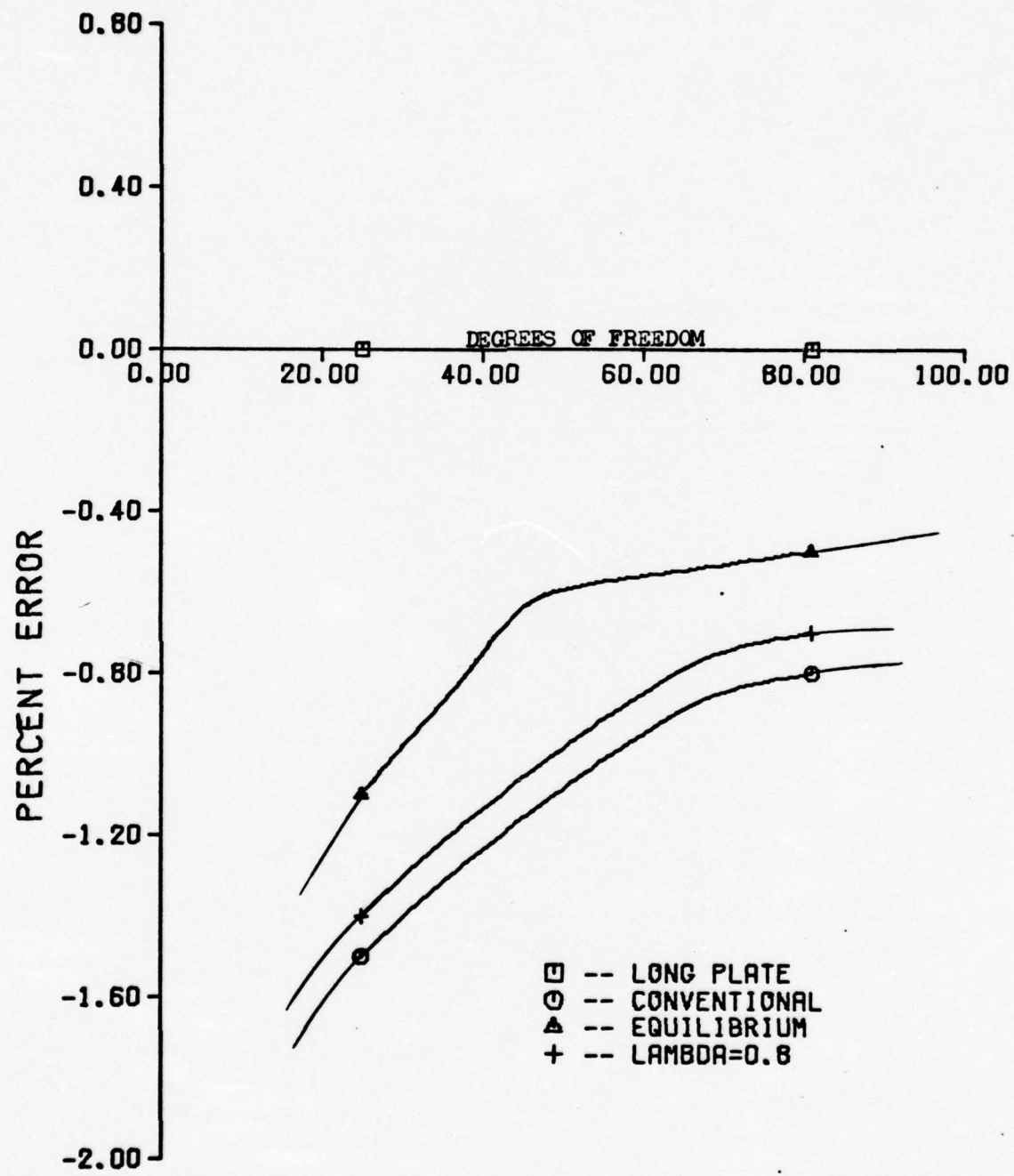


FIGURE 4.6 SIMPLE SUPPORTED PLATE $A/B=3.0$.

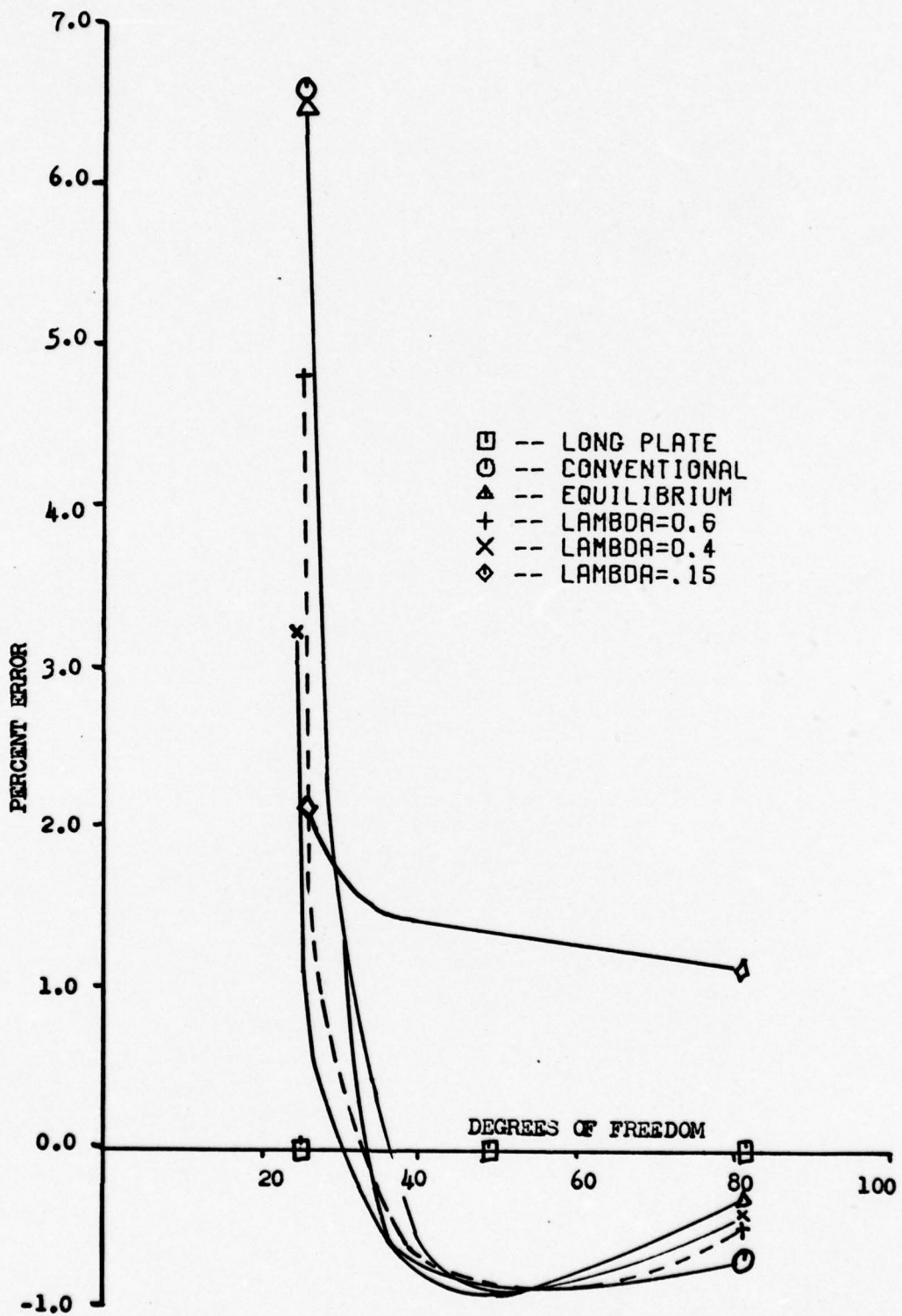


Figure 4.7 Simple Supported Plate A/B=5.0

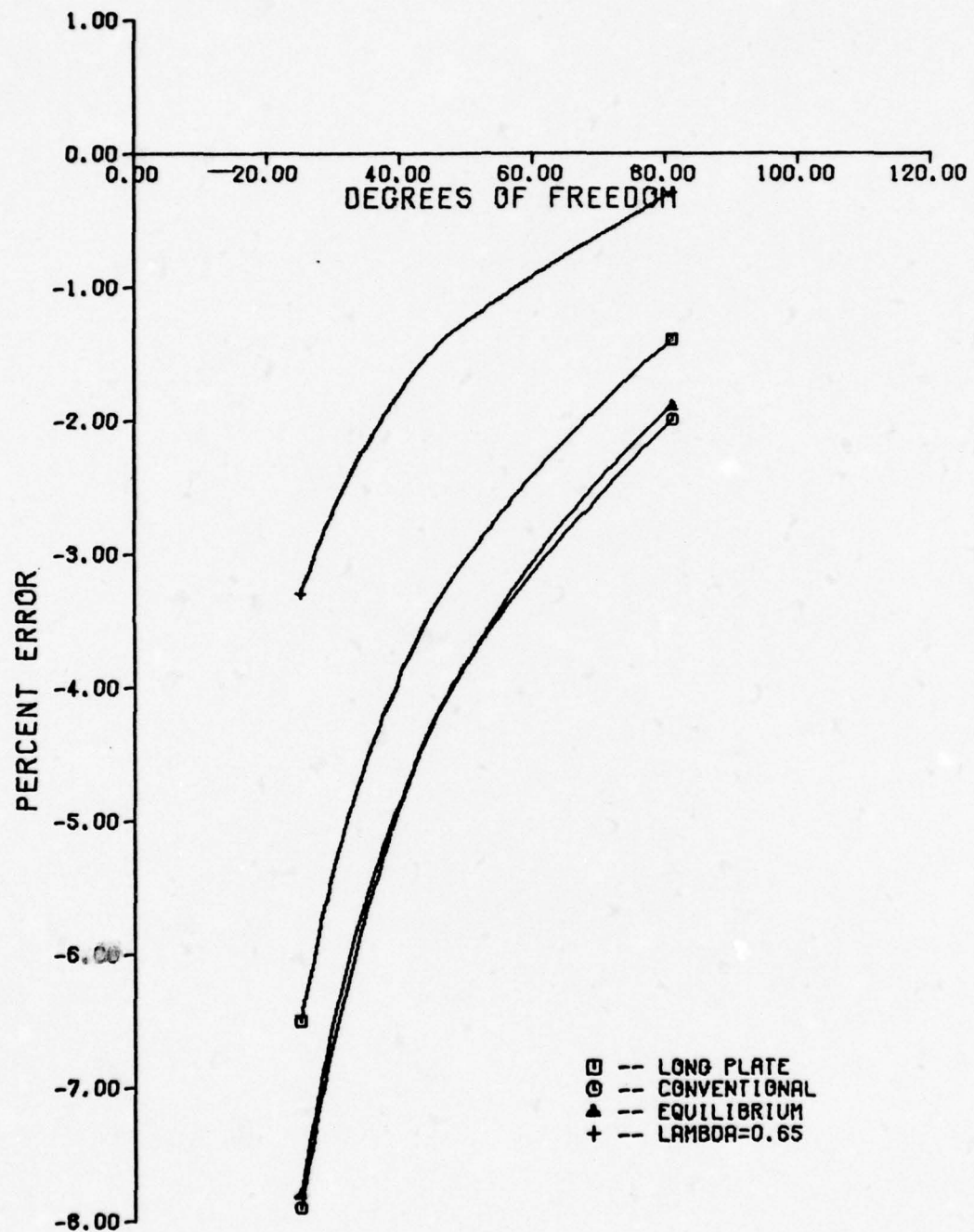


FIGURE 4.8 CLAMPED PLATE $A/B=0.5$

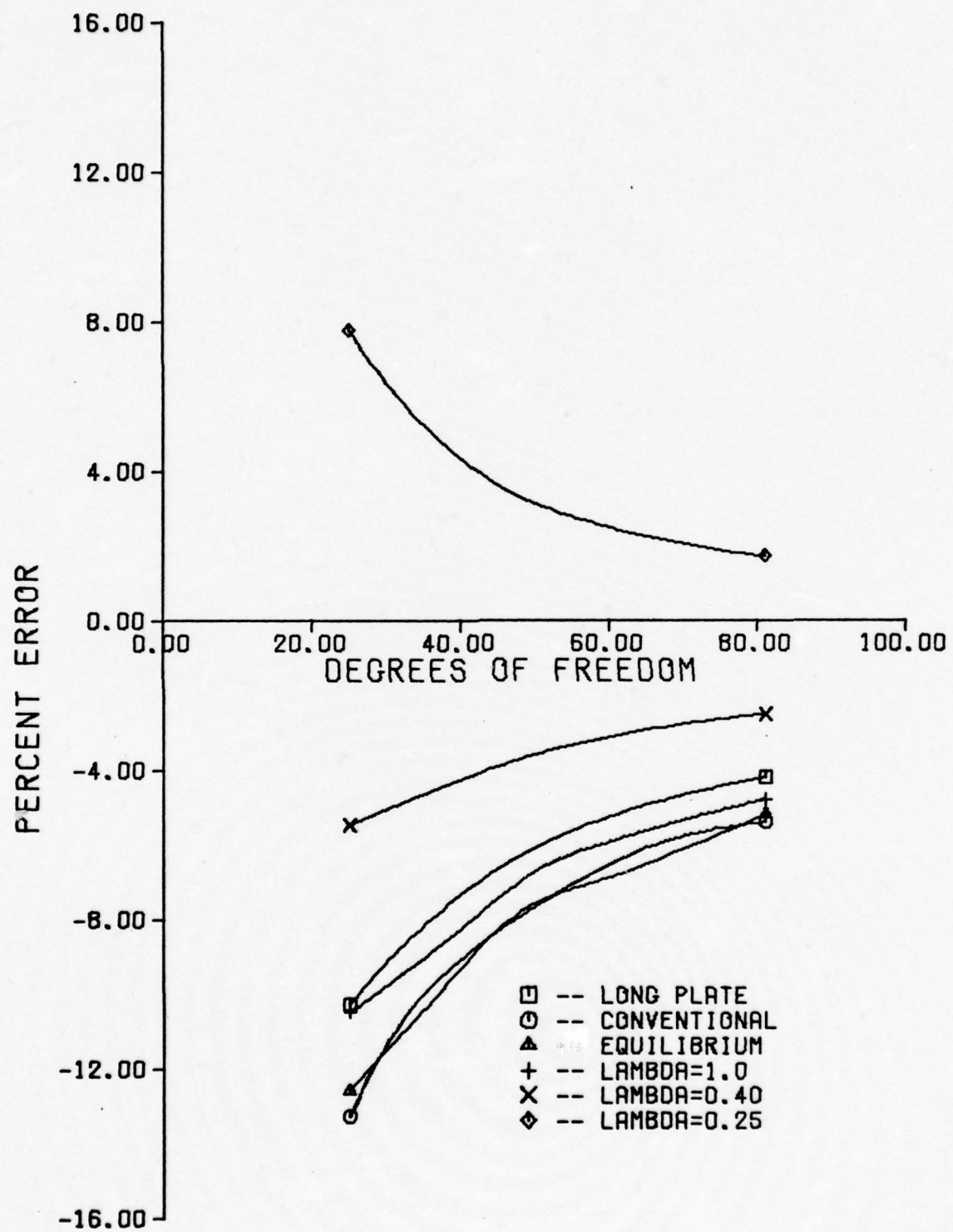


FIGURE 4.9 CLAMPED PLATE $A/B=1.0$

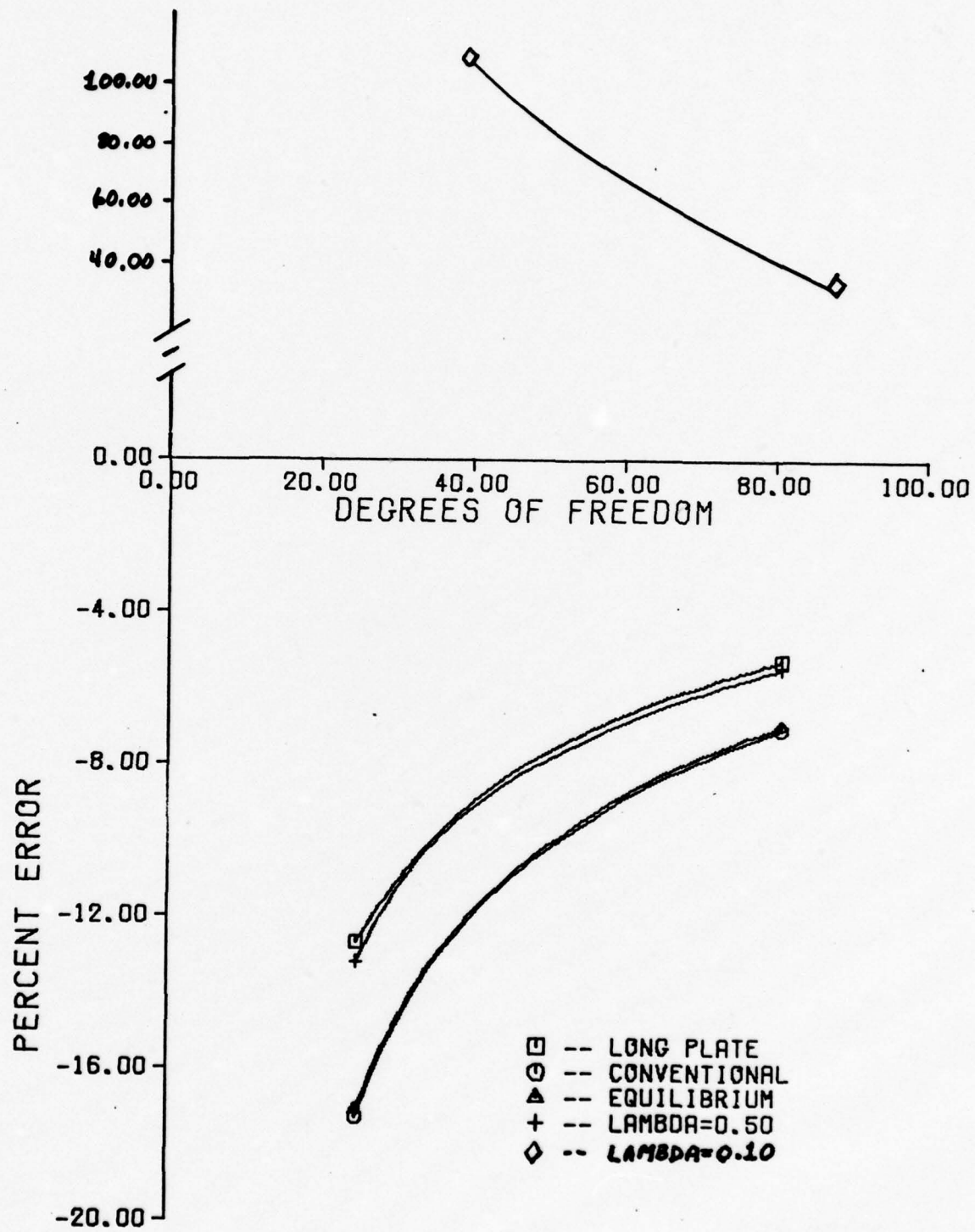


FIGURE 4.10 CLAMPED PLATE A/B=2.0

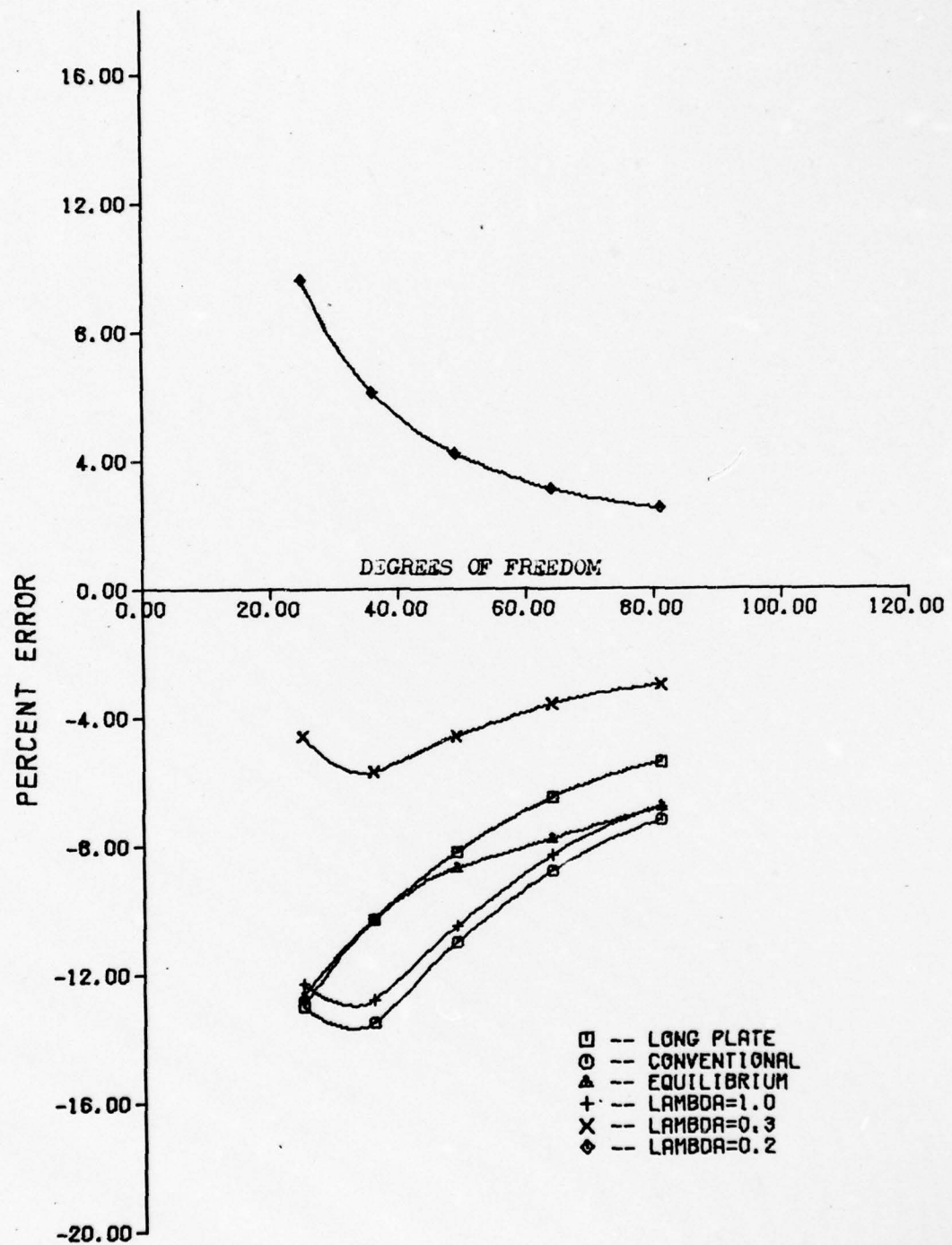


FIGURE 4.11 CLAMPED PLATE A/B=3.0

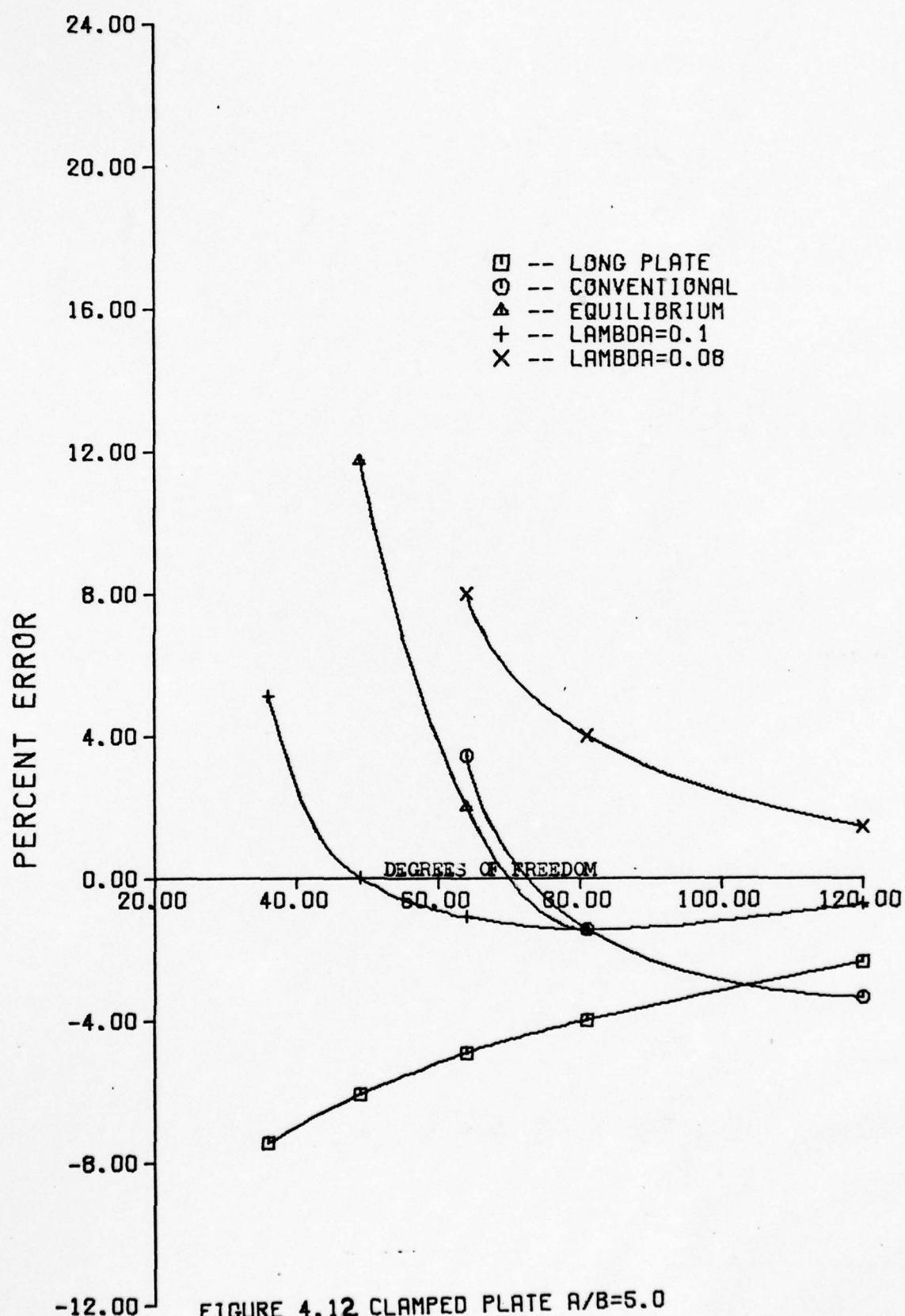


FIGURE 4.12 CLAMPED PLATE A/B=5.0

V. Conclusions

This thesis has compared results using expressions of virtual work and equilibrium, employing finite difference approximations, over a broad spectrum of aspect ratios for a buckling plate which was both simply supported and clamped. Little difference in accuracy was found between results obtained from conventional virtual work equation and the equilibrium equation. The virtual work method can be improved by incorporating into the finite difference expressions a trigonometric function using a buckled shape for a very long plate. In many instances certain selections of Lambda values lead to more accurate answers with the trigonometric approach.

Except for an aspect ratio of 5.0, all methods using simply supported plates were accurate and reliable at all degrees of freedom (25 or above). At an aspect ratio 5.0, inflections of the error function were encountered and some methods oscillated between stiff and flexible. The reason apparently is that large constant mesh sizes are not able to properly model the boundary conditions for long simply supported plates.

For clamped plates, buckling coefficient inaccuracies began to increase for aspect ratios as low as 1.0 and oscillation tendencies were encountered for aspect ratios of 3.0 and 5.0. Thus, the author feels that additional reasons for the inaccuracies and oscillations must be put

forth. They may be thought of as:

1. The inaccuracy encountered by approximating the boundary conditions in the basic virtual work equation with an insufficient number of node points adjacent to the boundary.
- and 2. The choice of a displacement function (referred to as Lambda) which doesn't satisfy the kinematic boundary conditions properly. (It should be noticed that the Lambda selection is very similar to choosing a displacement function for the Rayleigh-Ritz technique and though this thesis hasn't addressed all the ramifications of this comparison, several inaccuracies created through the use of various Lambda ratios have been mentioned.)

In essence, rapid convergence can be achieved by selecting a Lambda ratio which satisfies the boundary conditions. It should also be noted that since the function selected is incorporated into the finite difference approximation, accuracy can be maintained by using more degrees of freedom.

Bibliography

1. Stein, Manuel and Jerrold Housner. Numerical Analysis and Parametric Studies of the Buckling of Composite Orthotropic Compression and Shear Panels. NASA Technical Note D-7996, Washington: National Aeronautics and Space Administration, October 1975.
2. Gerard, George and H. Becker. Handbook of Structural Stability. Part II - Buckling of Flat Plates. NACA TN 3781, 1957.
3. Mansfield, E.H. The Bending and Stretching of Plates. New York: MacMillan Co., 1964.
4. Bryan, G.H. On the Stability of a Plane Plate Under Thrusts in Its Own Plane, With Applications to the "Buckling" of the Sides of a Ship. Proc. London Math Soc., Vol 22, Dec 11, 1890, pp. 54-67.
5. Almroth, B.O. and D.O. Brush. Buckling of Bars, Plates, and Shells. New York: McGraw-Hill Book Co., 1975.
6. Timoshenko, S.P. and S. Woinowsky-Krieger. Theory of Plates and Shells (Second Edition). New York: McGraw-Hill Book Co. Inc., 1959.
7. Timoshenko, S.P. and J.M. Gere. Theory of Elastic Stability (Second Edition). New York: McGraw-Hill Book Co., 1961.
8. Bleich, Friedrich. Buckling Strength of Metal Structures. New York: McGraw-Hill Book Co. Inc., 1952.
9. Fung, Y.C. and E.E. Sechler. Thin Shell Structures: Theory, Experiment and Design. Englewood Cliffs, New Jersey: Prentice-Hall Inc., 1974.
10. Ural, Oktay. Finite Element Method: Basic Concepts and Applications. New York: Intext Educational Publishers, 1973.
11. Zienkiewicz, O.C. The Finite Element Method in Engineering Science. London: McGraw-Hill, 1971.
12. Leissa, A.W., et al. "A Comparison of Approximate Methods for the Solution of Plate Bending Problems." AIAA Journal, Vol 7, No. 5:920-928 (May 1969).
13. Cox, H.L. The Buckling of Plates and Shells. New York: Pergamon Press Book, The MacMillan Co., 1963.

14. Cunningham, W.J. Non-Linear Analysis. New York: McGraw-Hill, 1958.
15. Saada, A.S. Elasticity: Theory and Applications. New York: Pergamon Press Inc., 1974.
16. Libove, Charles and S.B. Batdorf. A General Small-Deflection Theory for Flat Sandwich Plates. NACA Rep 899, 1948. (Supercedes NACA TN 1526.)
17. Stowell, E.Z. A Unified Theory of Plastic Buckling of Columns and Plates. NACA Rep. 898, 1948. (Supercedes NACA TN 1556.)
18. Salvadori, M.G. "Numerical Computation of Buckling Loads by Finite Differences." ASCE, Vol 116, Paper No. 2441: 590-624 (1951).
19. Wylie, C.R. Advanced Engineering Mathematics (Fourth Edition) New York: McGraw-Hill Book Co., 1975.
20. Salvadori, M.G. and Baron. Numerical Methods in Engineering. New Jersey: Prentice Hall, 1952.
21. Wah, T. and L.R. Calcote. Structural Analysis by Finite Difference Calculus. New York: Van Nostrand Reinhold Co., 1970.
22. Collatz, L. Functional Analysis and Numerical Mathematics. New York: Academic, 1966.
23. Forsythe, G.E. and W.R. Wasow. Finite-Difference Methods for Partial Differential Equations. New York: Wiley, 1960.
24. Noor, A.K. "Improved Multilocal Finite-Difference Variant for the Bending Analysis of Arbitrary Cylindrical Shells." University of South Wales, UNICIV Rep. R-63, 1971.
25. Buchnell, D. and B.O. Almroth. "Finite Difference Energy Method for Nonlinear Shell Analysis." J. Comput. Structures, Vol 1, pp 361-387, 1971.
26. Ghali, A. and A.M. Neville. Structural Analysis: A Unified Classical and Matrix Approach. Scranton, Pennsylvania: Intext Educational Publishers, 1972.
27. Szilard, R. Theory and Analysis of Plates: Classical and Numerical Methods. New Jersey: Prentice-Hall Inc., 1974.

28. Batdorf, S.B., M. Schildcront and M. Stein. "Critical Combinations of Shear and Longitudinal Direct Stress for Long Plates with Transverse Curvature." NACA, TN 1347, 1947.
29. Salvadori, M.G. "Numerical Computation of Buckling Loads by Finite Differences." ASCE Vol 116, Paper No. 2441, 1951.

Appendix A
Development of the Virtual
 Work Equation

The strain energy of a two-dimensional plate problem in terms of strain is

$$U = \int_V \frac{1}{2} \frac{E}{(1-v^2)} \left[e_x^2 + e_y^2 + 2v e_x e_y + \frac{1-v}{2} e_{xy}^2 \right] dv \quad (A1)$$

where the nonlinear strain-displacement relationships

$$\begin{aligned} e_x &= u_{,x} + \frac{1}{2}(w_{,x})^2 \\ e_y &= v_{,y} + \frac{1}{2}(w_{,y})^2 \\ e_{xy} &= u_{,y} + v_{,x} + w_{,x} w_{,y} \end{aligned} \quad (A2)$$

Equations (A2) are substituted into equation (A1) and then integrated over the thickness (t)

$$\begin{aligned} U &= \int_0^b \int_0^a \int_{-\frac{t}{2}}^{\frac{t}{2}} \frac{1}{2} \frac{E}{(1-v^2)} \left[[u_{,x} + \frac{1}{2}(w_{,x})^2]^2 + [v_{,y} + \frac{1}{2}(w_{,y})^2]^2 \right. \\ &\quad \left. + 2v [u_{,x} + \frac{1}{2}(w_{,x})^2] [v_{,y} + \frac{1}{2}(w_{,y})^2] \right. \\ &\quad \left. + \frac{1-v}{2} [u_{,y} + v_{,x} + w_{,x} w_{,y}]^2 \right] dz dx dy \end{aligned} \quad (A3)$$

if

$$\begin{aligned} u(x, y, z) &= -zw_{,x} \\ v(x, y, z) &= -zw_{,y} \\ w(x, y) &= w \quad (\text{no dependence on } z \text{ for small deflections in thin plates}) \end{aligned} \quad (A4)$$

The appropriate partials of equation (A3) are replaced with the above expressions yielding

$$U = \int_0^b \int_0^a \frac{t}{2} \frac{1}{2} \frac{E}{(1-u^2)} \left[z^2 w^2_{,xx} - zw_{,xx} w^2_{,x} + \frac{1}{4} w^4_{,x} + z^2 w^2_{,yy} - xw_{,yy} w^2_{,y} + \frac{1}{4} w^4_{,y} + 2u [z^2 w_{,xx} w_{,yy} - \frac{1}{2} zw_{,yy} w^2_{,x} - \frac{1}{2} zw_{,xx} w^2_{,y} + \frac{1}{4} w^2_{,x} w^2_{,y}] + \frac{1-u}{2} [z^2 w^2_{,xy} + 2z^2 w^2_{,xy} - 2zw_{,xy} w^2_{,x} w^2_{,y} + z^2 w^2_{,xy} - 2zw_{,xy} w^2_{,x} w^2_{,y}] \right] dz dx dy \quad (A5)$$

Equation (A5) is integrated with respect to z and combined yielding

$$U = \int_0^b \int_0^a \frac{1}{2} \frac{E}{(1-u^2)} \left[\frac{t^3}{12} w^2_{,xx} + \frac{t}{4} w^4_{,x} + \frac{t^3}{12} w^2_{,yy} + \frac{t}{4} w^4_{,y} + 2u \left[\frac{t^3}{12} w^2_{,xx} w_{,yy} + \frac{t}{4} w^2_{,x} w^2_{,y} \right] + \frac{1-u}{2} \left[\frac{t^3}{3} w^2_{,xy} + tw^2_{,x} w^2_{,y} \right] \right] dx dy \quad (A6)$$

The internal virtual work during buckling based on Eq. (A6) is

$$\delta U = \int_0^b \int_0^a \frac{1}{2} \frac{E}{(1-u^2)} \left[\frac{t^3}{6} w_{,xx} \delta w_{,xx} + tw^3_{,x} \delta w_{,x} + \frac{t^3}{6} w_{,yy} \delta w_{,yy} + tw^3_{,y} \delta w_{,y} + 2u \left[\frac{t^3}{12} w_{,yy} \delta w_{,xx} + \frac{t^3}{12} w_{,xx} \delta w_{,yy} + \frac{t}{2} w^2_{,x} w^2_{,y} \delta w_{,x} + \frac{t}{2} w^2_{,x} w^2_{,y} \delta w_{,y} \right] + \frac{1-u}{2} \left[\frac{2t^3}{3} w_{,xy} \delta w_{,xy} + 2tw_{,x} w^2_{,y} \delta w_{,x} + 2tw^2_{,x} w^2_{,y} \delta w_{,y} \right] \right] dx dy \quad (A7)$$

Like terms in w are combined

$$\delta U = \int_0^b \int_0^a \left[\frac{1}{12} \frac{Et^3}{(1-v^2)} [w_{xx} + vw_{yy}] \delta w_{xx} + \frac{1}{12} \frac{Et^3}{(1-v^2)} [w_{yy} + vw_{xx}] \delta w_{yy} + \frac{1}{6} \frac{Et^3}{(1+v)} w_{xy} \delta w_{xy} + \frac{Et}{2(1-v^2)} [w^3_{xx} + w^2_{xy} w^2_{yy}] \delta w_{xy} \right] dx dy \quad (A8)$$

If the higher order terms in equation (A8) are neglected, then the internal virtual work of a plate during buckling (specifically derived from nonlinear strain-displacement relationships, but representing linear strain expressions) becomes

$$\delta U = \int_0^b \int_0^a (M_x \delta w_{xx} + M_y \delta w_{yy} + 2M_{xy} \delta w_{xy}) dx dy \quad (A9)$$

where

$$\begin{aligned} M_x &= D_{11} w_{xx} + D_{12} w_{yy} \\ M_y &= D_{12} w_{xx} + D_{22} w_{yy} \\ M_{xy} &= 2D_{66} w_{xy} \end{aligned} \quad (A10)$$

and

$$\begin{aligned} D_{11} &= D_{22} = Et^3 / 12(1-v^2) \\ D_{12} &= vD_{11} \\ D_{66} &= Et^3 / 24(1+v) \end{aligned} \quad (A11)$$

The potential energy of the external forces is completely developed in Appendix D of [16] (Equations are shown

below for completeness). In their development it is pointed out that the middle surface stresses (N_x, N_y, N_{xy}) are assumed to remain unchanged in the course of the plate's deflection. This also implies that no middle surface stretching occurs during deflection, thus completely eliminating any nonlinear large strain effects. The total potential energy caused by in-plane external forces is

$$V = \frac{1}{2} \int_0^a \int_0^b [N_x w_{,x}^2 + N_y w_{,y}^2 + 2N_{xy} w_{,x} w_{,y}] dy dx \quad (A12)$$

The virtual work is then

$$\delta V = \frac{1}{2} \int_0^a \int_0^b [2N_x w_{,x} \delta w_{,x} + 2N_y w_{,y} \delta w_{,y} + 2N_{xy} w_{,x} \delta w_{,y} + 2N_{xy} w_{,y} \delta w_{,x}] dy dx$$

which reduces to

$$\delta V = \int_0^a \int_0^b (N_x w_{,x} \delta w_{,x} + N_y w_{,y} \delta w_{,y} + N_{xy} w_{,x} \delta w_{,y} + N_{xy} w_{,y} \delta w_{,x}) dy dx \quad (A13)$$

Equations (A9) and (A13) are combined.

This gives the virtual work equation used in this thesis.

$$\int_0^b \int_0^a (M_x \delta w_{,xx} + M_y \delta w_{,yy} + 2M_{xy} \delta w_{,xy}) dx dy = \int_0^a \int_0^b (N_x w_{,x} \delta w_{,x} + N_y w_{,y} \delta w_{,y} + N_{xy} w_{,x} \delta w_{,y}) dy dx \quad (A14)$$

Appendix B
Factoring Techniques

This particular Appendix is designed to show how numerical equations are ordered starting from the expression

$$\sum_{i=1}^M \sum_{j=1}^N (C_{ij} + A_{ij} N_x) \delta w_{ij} = 0 \quad (3-52)$$

An example using several grid points is presented to allow the reader a fuller appreciation of the numerical volume integration (Fig 3.4). For completeness, Equation (3-40) is repeated here in moment form.

$$\begin{aligned} \delta U = h_x h_y \sum_{i=1}^M \sum_{j=1}^N & \left[\xi_{x_i} \xi_{y_j} \left[D_{11} M_{x_{ij}} / \hat{h}_x^4 + D_{12} M_{y_{ij}} / \hat{h}_x^2 \hat{h}_y^2 \right] \right. \\ & \left[\delta w_{i+1,j} - 2\delta w_{ij} + \delta w_{i-1,j} \right] + \xi_{x_i} \xi_{y_j} \left[D_{12} M_{x_{ij}} / \hat{h}_y^2 \hat{h}_x^2 \right. \\ & \left. + D_{22} M_{y_{ij}} / \hat{h}_y^4 \right] \left[\delta w_{i,j+1} - 2\delta w_{ij} + \delta w_{i,j-1} \right] \\ & + 2n_{x_i} n_{y_j} \left[2D_{66} (w_{i+1,j+1} - w_{i,j+1} - w_{i+1,j} + w_{ij}) \right. \\ & \left. (\delta w_{i+1,j+1} - \delta w_{i,j+1} - \delta w_{i+1,j} + \delta w_{ij}) / \hat{h}_x^2 \hat{h}_y^2 \right] \end{aligned} \quad (B1)$$

and

$$\begin{aligned} \delta V = -h_x h_y \sum_{i=1}^M \sum_{j=1}^N & \left[\xi_{y_j} n_{x_i} N_x (w_{i+1,j} - w_{ij}) (\delta w_{i+1,j} \right. \\ & \left. - \delta w_{ij}) / \hat{h}_x^2 \right] \end{aligned} \quad (B2)$$

For simplicity let $M_{Y_{ij}} = M_{XY_{ij}} = D_{12} = D_{66} = 0$ thus

Equation (B1) with (B6) becomes

$$\sum_{i=1}^M \sum_{j=1}^N \left[\xi_{x_i} \xi_{y_j} \left[D_{11} M_{x_{ij}} / \hat{h}_x^4 \right] \left[\delta w_{i+1,j} - 2\delta w_{ij} + \delta w_{i-1,j} \right] \right] \\ + \left[\xi_{y_j} n_{x_i} N_x (w_{i+1,j} - w_{ij}) (\delta w_{i+1,j} - \delta w_{ij}) / \hat{h}_x^2 \right] = 0 \quad (B3)$$

If one rearranges and combines like terms the following is obtained

$$\sum_{i=1}^M \sum_{j=1}^N \left[\xi_{x_i} \xi_{y_j} D_{11} M_{x_{ij}} / \hat{h}_x^4 + \xi_{y_j} n_{x_i} N_x (w_{i+1,j} - w_{ij}) / \hat{h}_x^2 \right] \delta w_{i+1,j} \\ - \left[\xi_{x_i} \xi_{y_j} 2D_{11} M_{x_{ij}} / \hat{h}_x^4 + \xi_{y_j} n_{x_i} N_x (w_{i+1,j} - w_{ij}) / \hat{h}_x^2 \right] \delta w_{i+1,j} \\ + \left[\xi_{x_i} \xi_{y_j} D_{11} M_{x_{ij}} / \hat{h}_x^4 \right] \delta w_{i-1,j} = 0 \quad (B4)$$

Consider the terms $i=2, j=2$ identified as $\sum_{i=2}^{i=2} \sum_{j=2}^{j=2}$, and corresponding to grid point 7. From our boundary Equations (3-41) thru (3-44)

$$\sum_{i=2}^{i=2} \sum_{j=2}^{j=2} \xi_{x_2} = \frac{1}{2}, \quad \xi_{y_2} = \frac{1}{2}, \quad n_{x_2} = 1, \quad n_{y_2} = 1 \quad (B5)$$

Equation (B4) becomes

$$\begin{aligned}
& \dots + \sum_{i=2}^{\infty} \sum_{j=2}^{\infty} \left[\frac{1}{2} \cdot \frac{1}{2} D_{11} M_{x_7} / \hat{h}_x^4 + \frac{1}{2} \cdot 1 \cdot N_x (w_{12} - w_7) / \hat{h}_x^2 \right] \delta w_{12} \\
& - \left[\frac{1}{2} \cdot \frac{1}{2} \cdot 2 \cdot D_{11} M_{x_7} / \hat{h}_x^4 + \frac{1}{2} \cdot 1 \cdot N_x (w_{12} - w_7) / \hat{h}_x^2 \right] \delta w_7 \\
& + \left[\frac{1}{2} \cdot \frac{1}{2} D_{11} M_{x_7} / \hat{h}_x^4 \right] \delta w_2 \\
& + \sum_{i=2}^{\infty} \sum_{j=3}^{\infty} \left[\frac{1}{2} \cdot 1 \cdot D_{11} M_{x_8} / \hat{h}_x^4 + 1 \cdot 1 \cdot N_x (w_{13} - w_8) / \hat{h}_x^2 \right] \delta w_{13} \\
& - \left[\frac{1}{2} \cdot 1 \cdot 2 \cdot D_{11} M_{x_8} / \hat{h}_x^4 + 1 \cdot 1 \cdot N_x (w_{13} - w_8) / \hat{h}_x^2 \right] \delta w_8 \\
& + \left[\frac{1}{2} \cdot 1 \cdot D_{11} M_{x_8} / \hat{h}_x^4 \right] \delta w_3 + \dots + \dots + \dots + \\
& + \sum_{i=3}^{\infty} \sum_{j=2}^{\infty} \left[1 \cdot \frac{1}{2} \cdot D_{11} M_{x_{12}} / \hat{h}_x^4 + \frac{1}{2} \cdot 1 \cdot N_x (w_{17} - w_{12}) / \hat{h}_x^2 \right] \delta w_{17} \\
& - \left[1 \cdot \frac{1}{2} \cdot 2 \cdot D_{11} M_{x_{12}} / \hat{h}_x^4 + \frac{1}{2} \cdot 1 \cdot N_x (w_{17} - w_{12}) / \hat{h}_x^2 \right] \delta w_{12} \\
& + \left[1 \cdot \frac{1}{2} \cdot D_{11} M_{x_{12}} / \hat{h}_x^4 \right] \delta w_7 \\
& + \sum_{i=3}^{\infty} \sum_{j=3}^{\infty} \left[1 \cdot 1 \cdot D_{11} M_{x_{13}} / \hat{h}_x^4 + 1 \cdot 1 \cdot N_x (w_{18} - w_{13}) / \hat{h}_x^2 \right] \delta w_{18} \\
& - \left[1 \cdot 1 \cdot 2 \cdot D_{11} M_{x_{13}} / \hat{h}_x^4 + 1 \cdot 1 \cdot N_x (w_{18} - w_{13}) / \hat{h}_x^2 \right] \delta w_{13} \\
& + \left[1 \cdot 1 \cdot D_{11} M_{x_{13}} / \hat{h}_x^4 \right] \delta w_8 + \sum_{i=3}^{\infty} \sum_{j=4}^{\infty} \dots - \dots - \dots - \dots - \quad (B6)
\end{aligned}$$

Thus, as each term is evaluated the virtual displacements can gain coefficients as can be observed in Equation (B6) for δw_7 and δw_8 . After evaluating all the terms, the equation is reordered to gain a final coefficient matrix A and a virtual displacement vector δw_{ij} where the coefficient matrix A is composed of $C_{ij} + A_{ij} N_x$.

Vita

William Harold Deschler was born under the sign of Scorpio on November 13th 1944. He attended St. Joseph High School in Wapakoneta, Ohio. In 1964 he enlisted in the Air Force and spent a year at Indiana University learning Russian. After a tour of Japan with the Security Service, he was accepted into the Airman Education and Commissioning Program and obtained a Bachelor's Degree at Oklahoma State University in Mechanical Engineering. Pilot training at Williams AFB led to a Viet Nam assignment flying EC-47's. After that assignment he became a member of the Strategic Air Command and piloted the KC-135 aircraft. In 1975 he was accepted by the Air Force Institute of Technology. He obtained a Masters Degree in Aerospace Engineering and is presently assigned to the Foreign Technology Division in the Advanced Space Systems Branch.

Permanent Address: 1453 Town Hall Road

Dayton, Ohio 45432

A special thanks to my typist Mrs. Laura Reams.

Unclassified

SECURITY CLASSIFICATION OF THIS PAGE (When Data Entered)

REPORT DOCUMENTATION PAGE		READ INSTRUCTIONS BEFORE COMPLETING FORM
1. REPORT NUMBER GAE/MC/76D-3	2. GOVT ACCESSION NO.	3. RECIPIENT'S CATALOG NUMBER
4. TITLE (and Subtitle) COMPARING TRIGONOMETRIC AND CONVENTIONAL FINITE DIFFERENCE APPROXIMATIONS FOR PLATE BUCKLING		5. TYPE OF REPORT & PERIOD COVERED MA THESIS June 75 - Dec 76
7. AUTHOR(s) William H. Deschler Captain USAF		6. PERFORMING ORG. REPORT NUMBER
9. PERFORMING ORGANIZATION NAME AND ADDRESS Air Force Institute of Technology AFIT/EN Wright-Patterson AFB, Ohio 45433		10. PROGRAM ELEMENT, PROJECT, TASK AREA & WORK UNIT NUMBERS
11. CONTROLLING OFFICE NAME AND ADDRESS		12. REPORT DATE 10 December 76
		13. NUMBER OF PAGES 70
14. MONITORING AGENCY NAME & ADDRESS(if different from Controlling Office)		15. SECURITY CLASS. (of this report) Unclassified
		15a. DECLASSIFICATION/DOWNGRADING SCHEDULE
16. DISTRIBUTION STATEMENT (of this Report) Approved for public release, distribution unlimited.		
17. DISTRIBUTION STATEMENT (of the abstract entered in Block 20, if different from Report)		
18. SUPPLEMENTARY NOTES Approved for release; IAW AFR 190-17 JERRAL F. GUESS, USAF Director of Information		
19. KEY WORDS (Continue on reverse side if necessary and identify by block number) Finite Difference Theory Plates and Structures Buckling Numerical Analysis		
20. ABSTRACT (Continue on reverse side if necessary and identify by block number) Finite difference methods for plate buckling were investigated for various two-dimensional plates. The plates were clamped and simply supported. The rate of convergence to buckling coefficients, considering virtual work and equilibrium, have been compared. A trigonometric function (based on long plate theory) was incorporated into the finite difference approximations of the virtual work expression. Additional trigonometric parameters were also considered → next page		

Unclassified

SECURITY CLASSIFICATION OF THIS PAGE(When Data Entered)

→in the virtual work equation. Little difference in accuracy was found between results obtained from conventional (polynomial) virtual work versus the equilibrium approach. Noticeable improvement is obtained by using a trigonometric function (long plate assumption) in the virtual work expression. ←If one varies the trigonometric function (not based on long plate theory), a band of results is created from use of the virtual work equation. Inaccuracies occurred at low degrees of freedom, for clamped plates at all length to width ratios, due to insufficient representation of the boundaries. Two dominant reasons for poor boundary representation seem to be; large mesh size at low degrees of freedom (mesh sizes were held constant) and the trigonometric function (polynomial for conventional finite difference) failing to satisfy the kinematic boundary conditions.

Unclassified

SECURITY CLASSIFICATION OF THIS PAGE(When Data Entered)